

## ”SNe Ia twins for life” towards a precise determination of $H_0$

P. RUIZ-LAPUENTE<sup>1,2</sup> AND J.I. GONZÁLEZ HERNÁNDEZ<sup>3,4</sup>

<sup>1</sup>*Instituto de Física Fundamental, Consejo Superior de Investigaciones Científicas, c/. Serrano 121, E-28006, Madrid, Spain*

<sup>2</sup>*Institut de Ciències del Cosmos (UB-IEEC), c/. Martí i Franqués 1, E-08028, Barcelona, Spain*

<sup>3</sup>*Instituto de Astrofísica de Canarias, E-38200 La Laguna, Tenerife, Spain*

<sup>4</sup>*Universidad de La Laguna, Dept. Astrofísica, E38206 La Laguna, Tenerife, Spain*

### ABSTRACT

Here we present an approach to the measurement of extragalactic distances using twin SNe Ia, taken from the early down to the nebular phase. The approach is purely empirical, although we can give a theoretical background on why the method is reliable. By studying those twins in galaxies where peculiar velocities are relatively unimportant, we can tackle the  $H_0$  tension problem. Here we apply the method to the determination of the distances to NGC 7250 and NGC 2525, who hosted respectively SN 2013dy and SN 2018gv, twins of two different SNe Ia prototypes: SN 2013aa/ SN 2017cbv and SN2011fe. From the study of the SN 2013aa and SN 2017cbv twin pair, by comparing it with SN 2011fe and applying the difference between the SN 2013aa/2017cbv and the SN 2011fe class, we find as well a good estimate of the distance to NGC 5643. We have just started to measure distances with this method for the samples in Freedman et al. and Riess et al. There are differences in measured distances to the same galaxy using Cepheids or TRGBs. In this context of discrepancy, the ”twins for life ” method is very competitive because it can provide distance estimates with a modulus error of  $\sigma_\mu = 0.04$  mag. Our findings called for a revision of the distances measured with Cepheids in Riess et al. (2022). NGC 7250 and NGC 2525 needed better measurements with Cepheids. We have noticed that the Cepheids-based distance obtained with the *JWST* in Riess et al. (2024a) for NGC 5643 is in a good agreement with what we find, unlike their previous estimate in Riess et al. (2022). The Hubble tension can arise from the way in which the local SNe Ia sample is linked to the SNe Ia Hubble flow sample. A good calibration of SNe Ia in the local sample is needed and we have started to gather it. We also expect to apply the ”twin” SNe Ia comparison from the local sample to that in galaxies with  $z$

>0.02–0.03 well into the Hubble flow to obtain a reliable value for  $H_0$ . Those distant SNe Ia can be observed with the *ELT* or the *JWST*.

*Keywords:* Hubble constant, Supernovae, general; supernovae, Type Ia; Galaxy distances; Galaxies: M101, NGC 5643, NGC 7250, NGC 2525

## 1. INTRODUCTION

Type Ia supernovae (SNe Ia) at high  $z$  led to the discovery of the acceleration of the Universe (Riess et al. 1998; Perlmutter et al. 1999) and of the presence of a repulsive dynamical component that permeates it and accounts for such accelerated expansion. This component is known as dark energy and its nature is the subject of present and future research.

Apart from such endeavour in the field of very large  $z$  (see the latest developments in Rubin et al. 2023), there is, at low  $z$  a very important question to solve: the Hubble tension. This is a well known tension between the value of the Hubble constant  $H_0$  derived from the CMB by the *Planck* collaboration and that obtained, using Cepheids, by Riess and co-workers in their *SHOES* program. The CMB value of  $H_0 = 67.4 \pm 0.5$  km s<sup>-1</sup> Mpc<sup>-1</sup> (Planck Collaboration 2020) and the latest *SHOES* value of  $H_0 = 73.29 \pm 0.9$  km s<sup>-1</sup> Mpc<sup>-1</sup> (Murakami et al. 2023) have now a discrepancy at the 5.7  $\sigma$  level.

Such difference in  $H_0$  questions seriously the  $\Lambda$ CDM model and some authors claim the need of new physics in the early Universe to make the *Planck* value compatible with that derived by methods involving low- $z$  astrophysical distance indicators such as Cepheids (see Di Valentino et al. 2021 for a review). An exploration for a possible consistency of the CMB Planck data with the *SHOES*  $H_0$  has been done (see the early attempt by Bernal et al. 2016, for instance), but no consistent solution appears satisfactory (Efstathiou et al. 2023, amongst others).

The situation, however, is not completely clear, since there are methods that do not use Cepheids and predict values of  $H_0$  in-between those from *Planck* and from *SHOES*. So, using the *Tip of the Red Giant Branch (TRGB)* method, Freedman et al. (2019) found a value of  $H_0 = 69.8 \pm 0.8$  (stat)  $\pm 1.7$  (sys) km s<sup>-1</sup> Mpc<sup>-1</sup>. They noted a mean difference in galaxy moduli  $\mu^{TRGB} - \mu^{Ceph} = 0.059$  mag. They measured a scatter significantly larger for the distant galaxies than for the nearby ones, where it amounts to  $\pm 0.05$  mag only. More recently, Madore & Freedman (2024) note that the more-distant sample of galaxies has both larger scatter in the sample and systematically lower Cepheid distance moduli than their corresponding TRGB distance moduli. In the TRGB versus Cepheids comparison differences, one can see an average error in

the differences between moduli for the near and the far sample (lower or above 12.5 Mpc) of 0.100 and 0.103 mag, respectively, and a scatter of the data points around the mean of 0.068 and 0.152 mag, respectively. This analysis suggests that the errors on the nearby galaxies moduli are overestimated by 0.032 mag and the errors on the distant sample underestimated by 0.049 mag. Thus, the discrepancies need a deeper examination between the two methods. In the meanwhile, Anand et al. (2024) have examined the difference in distance moduli to two galaxies using *JWST* data and applying both the TRGB and the Cepheids approaches and find a better agreement between those distances. This path is worth to be extended to the 37 SNe Ia host galaxies used in distance determinations by Riess et al. (2022). Most recently, there has been a release of the results from *JWST* Cepheids, *JWST* TRGB stars and *JWST* JAGB (J-region Asymptotic Giant Branch) stars by Freedman et al. (2024) and a reevaluation by Riess et al. (2024b). The number of distances to galaxies obtained with the *JWST* is limited to 11. There is a better agreement between distances from both teams, but the  $H_0$  obtained by each of the methods differ substantially. One major surprise has been the value obtained by Freedman et al. (2024) with JAGBs, which basically suggests that there is no Hubble Tension. The three methods give different values for  $H_0$  in Freedman et al. (2024): from TRGB  $H_0 = 69.85 \pm 1.75$  (stat)  $\pm 1.54$  (sys), from Cepheids  $H_0 = 72.05 \pm 1.86$  (stat)  $\pm 3.10$  (sys), from JAGBs  $H_0 = 67.96 \pm 1.85$  (stat)  $\pm 1.90$  (sys). In this study the changes in  $H_0$  can be traced to different distance moduli from various methods. As mentioned in Freedman et al. (2024), the weighted (unweighted) mean difference between JAGB minus Cepheid distance moduli is  $0.086 \pm 0.028$  ( $0.083 \pm 0.031$ ) mag or 4 %. That can drive the change in the value of  $H_0$ . Though, the distances by Riess et al. (2022, 2024a,b) are now significantly closer to the distances obtained by *JWST* by Freedman et al. (2024), Riess et al (2024b) get very different numbers in their final  $H_0$ , those being for *JWST* Cepheids  $73.4 \pm 2.1$ , for *JWST* JAGBs is  $72.2 \pm 2.2$  and for *JWST* TRGBs  $72.1 \pm 2.2$  km s<sup>-1</sup> Mpc<sup>-1</sup>. The issue of why the final value by the two different collaborations differs has not been clarified yet. The differences arising from the various methods require a deeper research.

On the other hand, the sample of distances obtained by the *Surface Brightness Fluctuations (SBF)* method, dominated by early-type galaxies as required by the method, show a mean difference of  $\mu^{SFB} - \mu^{Ceph} = 0.07$  mag between the distances estimated using SFB and those using the Cepheid calibration (Khetan et al. 2021). A value of  $H_0 = 70.50 \pm 2.37$  (stat)  $\pm 3.38$  (sys) km s<sup>-1</sup> Mpc<sup>-1</sup> is derived in that paper. This, however, has been questioned by Blakeslee et al. (2021), obtaining an  $H_0$  around 73 km s<sup>-1</sup> Mpc<sup>-1</sup>.

In general, there are promising ideas to give an estimate of  $H_0$ , but different applications of the methods lead also to different results (see the review by Freedman & Madore 2023, for instance).

To determine the value of  $H_0$  from the distances to galaxies which are not yet in the Hubble flow, peculiar velocities must be considered. Kenworthy et al. (2022), studying the uncertainties in the peculiar velocities obtained by various models, bring  $H_0$  from the use of Cepheids in 35 extragalactic hosts to a range from 71.8 to 77  $\text{km s}^{-1} \text{Mpc}^{-1}$ . So the actual *SHOES* value for  $H_0$  becomes  $73.1^{+2.6}_{-2.3} \text{ km s}^{-1} \text{Mpc}^{-1}$ , at  $2.6\sigma$  tension with Planck. This is a two-rung distance ladder result which has considered previous small-scale galactic motions studies from Peterson et al. (2022) and additional corrections from large-scale structure.

The measurement of  $H_0$  with the Tip of the Red Giant Branch and Cepheids is centered in providing solid distances to galaxies at  $< 40 \text{ Mpc}$  and use another brighter distance indicator to reach the Hubble flow. With the advent of the *JWST*, it has been considered the possibility of reaching the Hubble flow ( $z \sim 0.02-0.03$ ) with TRGB/Cepheids or with the relatively new method J-Region Asymptotic Giant Branch (JAGB) that provides an intrinsically brighter standard candle. The data to go through this innovative path are still to be gathered. Up to the present, the most common way to obtain  $H_0$  using these methods is to establish TRGB, Cepheids or JAGB stars distances to Type Ia supernovae (SNIa) host galaxies in the local volume and then calibrate together those SNe Ia absolute magnitudes with SNe Ia in the Hubble flow. The SNe Ia calibration depends therefore on three rungs: Rung 1 is the calibration of TRGB/Cepheids (JAGBs) with local anchors, rung 2 refers to the calibration of the distance to SNe Ia host galaxies with the TRGB/Cepheids/JAGBs and rung 3 is the overall calibration of SNe Ia in the Hubble flow, which is done in different ways but usually involves the derivation of their absolute magnitudes in relation to  $H_0$  (see for instance Hamuy et al. 2021; Freedman et al. 2019). Hamuy et al. (2021) have found that the final  $H_0$  relies very much on the values of the distances to nearby host galaxies of SNe Ia using either the TRGB or the Cepheids method, i.e, on the second rung.

Here we address the distances to SNe Ia which constitute the basis for the  $H_0$  calibration in rung 2, i.e. in nearby galaxies that hosted SNe Ia. We compare them with the TRGB and Cepheids distances in those galaxies. We use the twinness of SNe Ia (see below) and hope, in the future, to reach  $H_0$  by directly allowing twin to twin SNe Ia comparison from nearby  $z$  up to  $z \sim 0.02-0.03$ .

The use of SNe Ia as distance indicators for cosmology was only made possible when the correlation between maximum brightness and rate of decline in the light curve was formulated in a general, quantitative way by Phillips (1993). Later on, further ways to formulate such correlation have been the stretch  $s$ , first introduced by Perlmutter et al. (1999), the *Multi Light Curves Shape (MLCSk2)* (Riess et al. 1996; Jha et al. 2007), or the stretch  $x1$  (Guy et al. 2005), which go beyond the parameterization by  $\Delta m_{15}$  (magnitude different between peak brightness and that 15 days later) of

the decline rate introduced by Phillips (1993). One current advance in achieving a more precise use of the rate of decline of the SNe Ia to standardize them is the inclusion of twin embedding (Fakhouri et al. 2015; Boone et al. 2016, 2021). It started when Fakhouri et al. (2015) found that by using SN Ia pairs with closely matching spectra, from the SNFactory sample, they achieved a reduced dispersion in brightness. They were able to standardize SNe Ia in the redshift range  $z$  between 0.03 and 0.08 to within 0.06–0.07 mag. The idea is most promising, given the expected massive gathering of SNe Ia spectra at high  $z$ . Twins are used there to connect the absolute magnitude estimate at maximum brightness with parameters corresponding to the spectral diversity of the SNe Ia. The method is as well suited for the time when dark energy is entering in the Hubble diagram, allowing to determine  $\Omega_M$  and  $\Omega_{DE}$ , as well as the equation of state of dark energy.

In the present paper we propose to use "SNe Ia twins for life", from early to the nebular phases<sup>1</sup>. It is a use of SNe Ia to address the Hubble tension issue which uses the spectral evolution of those SNe Ia which have not only similar stretch but identical features along the lifetime of the SNe Ia. The precision of the distance provided by those twins should be larger than for SNe Ia with just similar stretch.

The method does not start from the apparent magnitudes of the SNe Ia, but from their spectra, with particular emphasis on those from the nebular phase, which are very sensitive to the reddening and to the intrinsic luminosity of the SNe. To get a direct check of the distance ladder, we make an empirical use of twin SNe Ia by comparing their spectra all the way from the early until the nebular phase. We obtain a good estimate of the relative distances between SNe Ia which are in different galaxies but seem identical spectroscopically, in addition to having a similar stretch. It is important, here, that the SNe Ia do show twin behaviour through the SN Ia life. Given the range of diversity of the SNe Ia already sampled, it should always be possible to find some of them with spectra similar to those of any newly discovered SN Ia. As nearby SNe Ia will be observed by the thousands per month with the advent of more SNe Ia dedicated surveys with new telescopes together with the present ones, it will be possibly to match their spectra with those of distant SNe Ia and then gain a new perspective on the extragalactic distance scale. Extending this procedure to reach SNe Ia that are in the Hubble flow should allow to avoid using a fiducial absolute magnitude  $M_B$ – $H_0$  relation, and get a direct comparison of distances leading straightforwardly to the value of  $H_0$ . This would be very useful in helping to solve the Hubble tension problem.

<sup>1</sup> For those readers that are not familiar with SNe Ia phases, we clarify here that early phases are those next to maximum brightness, i.e, from -17 days to +15 days around the peak of brightness; nebular phases are those typically corresponding to more than 200 days after maximum, and the phase between maximum until the nebular phase corresponds to the evolution from early to late times, often simply called postmaximum or denoted by the epoch.

The gain of using the "twins for life" approach is that it provides a direct measurement of distance, intrinsic color and reddening caused by Galactic and extragalactic dust by the use of the whole spectra of the SN Ia. It allows the consistent pairing of SNe Ia through all phases. The selection of twins is made of SNe Ia with a similar stretch, being then of similar luminosities, but in addition the "twinness factor" can make more precise the distance estimate with a modulus error of 0.04 mag in all filters, as we will show. So, all this makes a very useful tool to gather the right distance ladder.

Twins allow to determine distances to SNe Ia host galaxies both in relation one to another in a relative scale and in absolute scale using well calibrated distances from recent nearby normal SNe Ia like SN 2011fe in M101. At present, there is no coincidence on distances to a nearby galaxy like M101, but there is progress in that direction. One can, in the meanwhile, aim towards a first step in the distance ladder by a choice of concordance between methods as Cepheids with *JWST* data, Miras distances, TRGB, JAGB stars, knowledge from constraints on very nearby SNe Ia or through a choice of some other method. We will address this in some subsections. At low distances like that of M101, the difference between methods is much smaller than at much larger distances where some of those methods can only get an accurate result with *JWST* data.

In section 2, we describe the method and characterize what is a perfect twin against other ways to compare SNe Ia. In section 3, we obtain the distance to NGC 7250, the host galaxy of SN 2013dy. In section 4, we obtain the distance to NGC NGC 2525, the host galaxy of SN 2018gv. In section 5 we compare our results within the SNe Ia diversity and discuss them. In section 6 we give our conclusions.

## 2. PURELY EMPIRICAL TWINS UNTIL THE NEBULAR PHASE

The key to this approach is to have a nearby SN Ia of the same type as another at much longer distance. For the nearby SN Ia, a good distance determination should be available. We will demonstrate this by using SN 2013dy in NGC 7250, which is a twin of SN2017cbv/SN2013aa both in NGC 5643.

Table 1 show the references for the spectra and photometry used in this paper. Some spectra have been provided generously by various researchers, and some others have been taken from the *WISeREP*. All are carefully calibrated in flux in agreement with the published photometry. The error in the flux calibration is well taken into account.

We first check the method by taking two twin SNe Ia that are at the same distance and share the same reddening: SN 2017cbv/SN 2013aa.

### 2.1. Testing the method with twin SNe Ia in NGC 5643

**Table 1.** Spectra and photometry of the SNe Ia twins sample

| <b>Spectra</b>    |          |       |              |                       |             |  |
|-------------------|----------|-------|--------------|-----------------------|-------------|--|
| SN                | Galaxy   | MJD   | Phase (days) | Reference*            | Comments    |  |
| 2013aa            | NGC 5643 | 56341 | -2           | Burns et al. (2020)   | Priv. comm. |  |
| ...               | ...      | 56391 | +48          | *                     |             |  |
| ...               | ...      | 56676 | +333         | *                     |             |  |
| ...               | ...      | 56704 | +361         | *                     |             |  |
| 2017cbv           | NGC 5643 | 57836 | -2           | Burns et al. (2020)   | Priv. comm. |  |
| ...               | ...      | 57848 | +12          | *                     |             |  |
| ...               | ...      | 58171 | +333         | *                     |             |  |
| ...               | ...      | 58199 | +361         | *                     |             |  |
| 2013dy            | NGC 7250 | 56498 | -2           | Pan et al. (2015)     |             |  |
| ...               | ...      | 56546 | +46          | Zhai et al. (2016)    |             |  |
| ...               | ...      | 56833 | +333         | Zhai et al. (2016)    |             |  |
| 2011fe            | M101     | 55823 | +9           | Zhang et al. (2016)   |             |  |
| ...               | ...      | 55826 | +12          | *                     |             |  |
| ...               | ...      | 56103 | +289         | Mazzali et al. (2015) |             |  |
| ...               | ...      | 56158 | +344         | *                     |             |  |
| 2018gv            | NGC 2525 | 58159 | +9           | *                     |             |  |
| ...               | ...      | 58439 | +289         | Graham et al. (2022)  | Priv. comm. |  |
| ...               | ...      | 58494 | +344         | Graham et al. (2022)  | Priv. comm. |  |
| <b>Photometry</b> |          |       |              |                       |             |  |
| 2013aa            | —        | —     | —            | Burns et al. (2020)   | —           |  |
| 2017cbv           | —        | —     | —            | Burns et al. (2020)   | —           |  |
| 2013dy            | —        | —     | —            | Pan et al. (2015)     | —           |  |
| 2011fe            | —        | —     | —            | Zhang et al. (2016)   | —           |  |
| 2018gv            | —        | —     | —            | Scolnic et al. (2022) | —           |  |

\* Spectrum from the *WISeREP*.

SN 2013aa and SN 2017cbv appeared in the same galaxy, NGC 5643. They had similar decline rates and similar B-peak magnitudes. The studies done on these two SNe Ia also reveal similar characteristics in other aspects. Table 1 specifies the decline rates of those SNe Ia not only by  $\Delta m_{15}(B)$  but also by  $s_{BV}^D$  (Burns et al. 2020).

Burns et al. (2014) showed that the color-stretch parameter is a robust way to classify SNe Ia in terms of light-curve shape and intrinsic colors. They propose a way to quantify the decline rate of the SNe directly from photometry, by just determining the epoch when the B–V color curves reach their maxima (i.e., when the SNe are reddest) relative to that of the B-band maximum. Dividing this time interval by 30 days then gives the observed color-stretch parameter  $s_{BV}^D$ . the “D” in the superindex referring to the direct comparison in B, without having to take into account the BVRI light curves.

**Table 2.** SN 2013aa and SN 2017cbv

|  |              |                  |
|--|--------------|------------------|
| <b>SN 2013aa</b>                               |              |                  |
| RA, DEC <sup>a</sup>                           | 14:32:33.881 | -44:13:27.80     |
| Discovery date <sup>a</sup>                    | ...          | 2013-02-13       |
| Phase (referred to maximum light) <sup>b</sup> | ...          | -7 days          |
| Redshift <sup>c</sup>                          | ...          | 0.004            |
| E(B-V) <sub>MW</sub> <sup>d</sup>              | ...          | 0.15±0.06 mag    |
| $m_B^{max}$ <sup>b</sup>                       | ...          | 11.094±0.003 mag |
| $\Delta m(B)_{15}$ <sup>b</sup>                | ...          | 0.95±0.01        |
| Stretch factor $s_{BV}^D$ <sup>b</sup>         | ...          | 1.11±0.02        |
| Phases of the spectra used                     | ...          | -2, 360-370 days |
| <b>SN 2017cbv</b>                              |              |                  |
| RA, DEC <sup>e</sup>                           | 14:32:34.420 | -44:08:02.74     |
| Discovery date <sup>e</sup>                    | ...          | 2017-03-10       |
| Phase (referred to maximum light) <sup>b</sup> | ...          | -18 days         |
| Redshift <sup>c</sup>                          | ...          | 0.004            |
| E(B-V) <sub>MW</sub> <sup>d</sup>              | ...          | 0.15±0.06 mag    |
| $m_B^{max}$ <sup>b</sup>                       | ...          | 11.11±0.03 mag   |
| $\Delta m(B)_{15}$ <sup>b</sup>                | ...          | 0.96±0.02        |
| Stretch factor $s_{BV}^D$ <sup>b</sup>         | ...          | 1.11±0.03        |
| Phases of the spectra used                     | ...          | -2, 360-370 days |

<sup>a</sup>Waagen (2013).<sup>b</sup>Burns et al. (2020).<sup>c</sup>Parrent et al. (2013).<sup>d</sup>Schlafly & Finkbeiner (2011).<sup>e</sup>Tartaglia et al. (2017).

The problems involved in the use of  $\Delta m_{15}(B)$  are known. The first one is that the decline in 15 days past maximum can take (and it often does) differing values in different authors. Phillips et al. (1999), noted in addition that any reddening undergone by the SN would change the shape of the B-band light-curve and therefore the observed value of  $\Delta m(B)_{15}$ . A similar problem is that, by definition,  $\Delta m(B)_{15}$  is tied to a particular photometric system, and so will vary from data set to data set and will require S-corrections (Suntzeff et al. 1988; Stritzinger et al. 2002) to convert one set of  $\Delta m_{15}(B)$  to another. And lastly,  $\Delta m(B)_{15}$  is defined by measuring the light curve at two very specific epochs, and some form of interpolation is usually needed to obtain these values.

Fitting the B-V color curves with cubic splines, Burns et al (2020) find identical color-stretch  $s_{BV}^D = 1.11$  for SN 2013aa and SN 2017cbv. This value is smaller (slower decline) than in typical SNe Ia. They also found similar values in the *Branch classification*, concerning the equivalent widths (EW) of the lines of different elements. This proves that their interior was very alike in chemical composition.

SN 2013aa and SN 2017cbv present a unique opportunity to test the method, by checking whether it gives any difference in the distance moduli of these two SNe Ia, using early and nebular spectra together. Both happened in NGC 5643. They were in the outskirts of the host galaxy, so the reddening E(B-V) there should be negligible.



The reddening in our Galaxy, in the direction of NGC 5643, is  $(E - B)_{MW} = 0.15$  mag, from Schlafly & Finkbeiner (2011). The properties of these two SNe Ia can be found in Table 2.

## 2.2. Methodology

The method to determine the relative distance  $\Delta\mu$  between the two SNe Ia will also give the relative reddening  $\Delta E(B - V)$ . Its value will indicate whether  $E(B - V)$  is larger or smaller for one of the two SNe with respect to its twin, taken as reference. The result in  $\Delta\mu$  indicates the difference in distance between that SN and the reference. The twin of reference is ideally a SN Ia for which the distance is well known. It has the role of anchor.

In the present case, we take as reference any of the twins. We do not need to know its distance: the result should point to a  $\Delta\mu \sim 0$  anyway. We will compare SN 2013aa with respect to the class represented by SN 2017cbv. The two phases taken into account are -2 days before and 361 days after B-maximum. Both SNe Ia happened in the outskirts of the same galaxy, NGC 5643, thus having negligible reddening in the host galaxy.

To find the best values and the uncertainties of all variables, we explore the parameter space with Markov Chain Monte Carlo (MCMC) techniques after converting the  $\chi^2$  into a log likelihood function:

$$\log\mathcal{L} = -0.5 * \sum (f_{\lambda}^{obs} - f_{\lambda}^{ref})^2 / \sigma_{\lambda}^2 + \log\sigma_{\lambda} \quad (1)$$

where *obs* corresponds to a given supernova and *ref* to its reference twin, which represents a whole class.  $f_{\lambda}^{obs}$  and  $f_{\lambda}^{ref}$  correspond to the fluxes of the two SNe at different wavelengths, and  $\sigma_{\lambda}$  includes the quadratic addition of the uncertainty on the fluxes of both SNe.

In fact, as we are using different phases, we have a total likelihood function. For two phases,  $n$  corresponds to 1 and 2 below. Thus the total likelihood function is written as

$$\log\mathcal{L}_n = \log\mathcal{L}_1 + \log\mathcal{L}_2 \quad (2)$$

i.e. just the addition of all individual SN phases.

We use a Python package, EMCEE (Foreman–Mackey et al. 2013)<sup>2</sup> to explore the likelihood of each variable. EMCEE utilizes an affine invariant MCMC ensemble sampler proposed by Goodman & Weare (2010). This sampler tunes only two parameters

<sup>2</sup> <https://emcee.readthedocs.io/>

to get the desired output: number of walkers and number of steps. The run starts by assigning initial maximum likelihood values of the variables to the walkers. The walkers then start wandering and explore the full posterior distribution. After an initial run, we inspect the samplers for their performance. We do this by looking at the time series of variables in the chain and computing the autocorrelation time,  $\tau^3$ . In our case, the maximum autocorrelation time among the different variables is about 50. When the chains are sufficiently burnt-in (e.g., they forget their initial start point), we can safely throw away some steps that are a few times higher than the burnt-in steps. In our case, we run EMCEE with 32 walkers and 10,000 steps and throw away the first  $\sim 250$  samples, equivalent to  $\sim 4$  times the maximum autocorrelation time. Thus, our burn-in value in this computation is equal to 4 times the maximum autocorrelation time. A criterion of good sampling is the acceptance fraction,  $a_f$ . This is the fraction of steps that are accepted after the sampling is done. The suggested value of  $a_f$  is between 0.2 - 0.5 (Gelman et al. 1996). In each run, we typically obtained  $a_f \sim 0.25$ .

We adopt uniform priors on the distance  $\Delta\mu(\mathcal{U}[-0.3,0.3])$  mag and reddening  $\Delta E(B - V)(\mathcal{U}[0.0,0.3])$  mag.

One can visualize the output of two-dimensional and one-dimensional posterior probability distributions in a corner plot corresponding to  $1\sigma$ ,  $2\sigma$ ,  $3\sigma$ . The results point to  $\Delta E(B - V) = 0.0 \pm 0.0$ , as it should have been expected from the two SNe being in the same galaxy with similar conditions of negligible reddening in the host galaxy and same reddening by dust in our Galaxy, and a  $\Delta\mu$  of  $0.004 \pm 0.005$  in the early spectrum and  $\mu = -0.023^{+0.008}_{-0.007}$  in the nebular one. Those correspond to a precision of 23 kpc for the early spectrum and around 100 kpc for the late one. In this plot, both the early and the late-time spectra are used. It is expected that individual fits will show their own errors. Separate comparisons for the two different phases are shown in Figure 1 and Figure 2. A joint comparison is seen in Figure 3. The joint comparison allows to see what happens if the various epochs are fitted together.  $\Delta\mu = -0.005 \pm 0.004$ , if we fit together the two phases.

The preceding demonstrates very successfully the possibility to combine early and late phase information to obtain relative distances or differences in distance moduli between the hosts of twin SNe Ia.

SN 2013aa and SN 2017cbv are their own SN Ia subclass. SN 2013dy belongs to that class of twinness.

In order to estimate the magnitude accuracy that twins have in their spectral comparison, we calculate the difference in the various filters B, V,R, I of the twin spectra

<sup>3</sup> <https://emcee.readthedocs.io/en/stable/tutorials/autocorr/>

at the same phase once they are shifted to a same distance (this same distance is calculated given the information provided by our emcee computation). The error estimate is of  $\sigma = 0.04$  in all filters and all phases. We have done the comparison not only with SN 2017cbv and SN 2013aa, but also with SN 2013dy. In all cases, the above  $\sigma$  is found. This confirms the power of this method to disentangle errors in SNe Ia host galaxies distances provided by TRGB, Cepheids, JAGB. The "twins for life" method is very competitive.

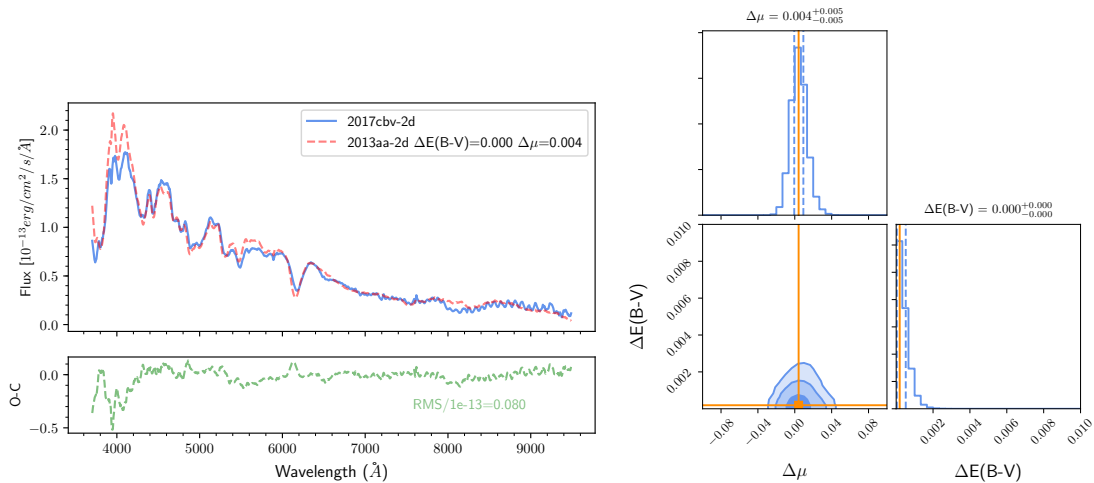


**Figure 1.** Left: Comparison of early time spectra of SN 2013aa and SN 2017cbv at -2 days before maximum light. Right:  $1\sigma$ ,  $2\sigma$  and  $3\sigma$  contours for the posterior probability distribution. The dashed vertical values correspond to  $1\sigma$  error in each variable.

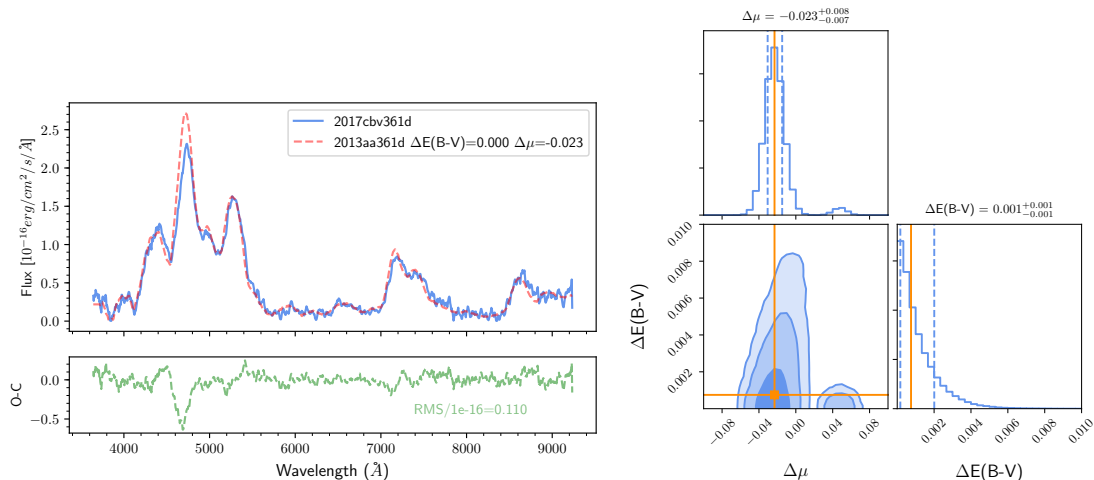


**Figure 2.** Left: Comparison of late-time spectra of SN 2013aa and SN 2017cbv at 361 days past maximum light. Right: As in Figure 1 but for the 361 days phase.

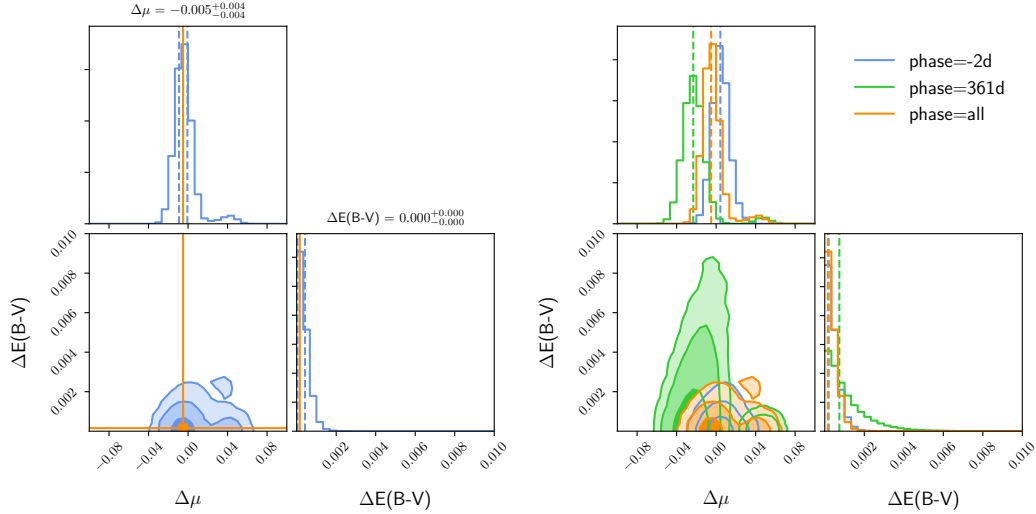


**Figure 3.** Left: Final joint result from early (-2d) and late time spectra (361d) of SN 2013aa and SN 2017cbv. Right: The results showing the corner plots with the  $1\sigma$ ,  $2\sigma$  and  $3\sigma$  confidence regions favored by each phase and those from the joint computation.

NGC 5643 will eventually become an important step of reference in the distance ladder for supernovae belonging to the class of twins of SN 2017cbv/SN 2013aa, hopefully reaching high enough  $z$ , where peculiar velocities do no longer prevent to reliably derive  $H_0$ .

### 2.3. Quantities that describe twin SNe Ia

Twin spectra of SNe Ia near maximum should have a similar shape of the pseudo-continuum and similar pseudo-equivalent widths (pWs) of the different lines. All that is required because otherwise it is not possible to have a difference in magnitude of  $\sigma = 0.04$  in all filters.

Other approaches that aim at addressing the similarity between spectra use a quantification that mixes various lines to map the space of spectral diversity (Fakhouri et al. 2015; Boone et al. 2016). In our case, we want to give values of the most relevant lines that characterize the physics of SNe Ia. Along this path, we study the place where the different pWs of the lines fall in diagrams such as those in Morrell et al. (2024).

We have measured lines relevant for describing the similarity of the spectra. The spectra of the twins have very similar pseudo-equivalent widths (pWs) in the list of lines called (see Morrell et al. 2024) pW1 (Ca H & K), pW2 (Si II  $\lambda$  4130 Å), pW3 (Mg  $\lambda$  4481; blended with Fe II), pW4 (Fe II at  $\sim$  4600 Å blended SII), pW5 (S II "W"  $\sim$  5400 Å), pW6 (Si II  $\lambda$  5972 Å), pW7 (Si II  $\lambda$  6355 Å), pW8 (Ca II IR Å). In particular, the line associated with Si II  $\lambda$  5972 Å should be very similar in

twin SNe Ia, with a discrepancy of less than 5%. This line correlates with stretch ( $\Delta m(B)_{15, s_{BV}}$ ), and amongst SNe Ia of similar stretch, has to be almost the same for twins. In the pW6 over pW7 diagram the twins should fall in very close positions.

If the equivalent widths are similar, the ratios of the to Si II at  $\lambda$  5972 Å and  $\lambda$  6355 Å  $\mathcal{R}_{SiII}$  should coincide.

The shape of the pseudo-continuum should point to a similar  $T_{\text{eff}}$  in order to overlap.

In the nebular phase, the presence of stable Ni lines should be similar as well as the width and relevance of the lines.

In Appendix A we present these checks on SN 2017cbv/SN 2013aa and SN 2011fe.

### 3. THE DISTANCE TO NGC 7250

SN 2013dy in NGC 7250 has a decline rate similar to that of SN 2013aa and SN 2018cbv. We have found enough similarities to suggest that it belongs to the class of twins represented by SN 2017cbv and SN 2013aa. It follows an evolution identical to those SNe Ia. The characteristics of this SN Ia can be found in Table 3.

SN 2013dy was discovered a few hours after explosion. This circumstance made possible a very intense photometric and spectroscopic follow up of this SN Ia (Pan et al. 2015). This supernova belongs to normal SNe Ia which can be fitted with a W7 type model with solar metallicity (Nomoto et al. 1984).

We went further looking for differences and similitudes with the two twin SNe Ia in NGC 5643. We were suprised to see the similarities in spectral evolution. We have selected three epochs to display this similitude: 2 days before maximum, 46 days after maximum and 333 days after maximum.

SN 2013dy is practically equal at late phases to SN 2017cbv (there are no spectra of SN 2013aa at that phase to allow a comparison). At very early phase it is similar to both SN 2017cbv and SN 2013aa though slightly redder. After maximum brightness is also identical to SN 2013aa.

Pan et al. (2015) show a comparison of the UV flux of SN 2013dy with that of SN 2011fe. The larger flux in SN 2013dy is consistent with a larger amount of  $^{56}\text{Ni}$  than for SN 2011fe. So it is its longer rise to B maximum, which is 17.7 days in SN 2013dy against 17.6 days in SN 2011fe.

SN 2013dy had significant reddening. The reddening in the Galaxy is  $E(B-V)_{MW} = 0.14$  mag (Schlafly & Finkbeiner 2011), though there are indications that the total

reddening might be higher with a possible lower  $R_V$  than 3.1. We will address this once we made our comparison of SN 2013dy with SN 2017cbv and SN 2013aa, those last ones reddened with a  $E(B-V)_{MW}=0.15$  mag (Schlafly & Finkbeiner 2011).

**Table 3.** SN 2013dy

| SN 2013dy                                      |              |                        |
|--|--------------|------------------------|
| RA, DEC <sup>a</sup>                           | 22:18:17.599 | +40:34:09.59           |
| Discovery date <sup>a</sup>                    | ...          | 2013-07-10             |
| Phase (referred to maximum light) <sup>b</sup> | ...          | -18 days               |
| Redshift <sup>c</sup>                          | ...          | 0.0039                 |
| $E(B-V)_{MW}$ <sup>d</sup>                     | ...          | 0.15 mag               |
| $m_B^{max}$ <sup>e</sup>                       | ...          | $13.229 \pm 0.010$ mag |
| $\Delta m(B)_{15}$ <sup>e</sup>                | ...          | $0.92 \pm 0.006$ mag   |
| Phases of the spectra used                     | ...          | -2, 46, 333 days       |

<sup>a</sup>Casper et al. (2013).

<sup>b</sup>Zheng et al. (2013).

<sup>c</sup>Schneider et al. (1992).

<sup>d</sup>Schlafly & Finkbeiner (2011).

<sup>e</sup>Pan et al. (2015).

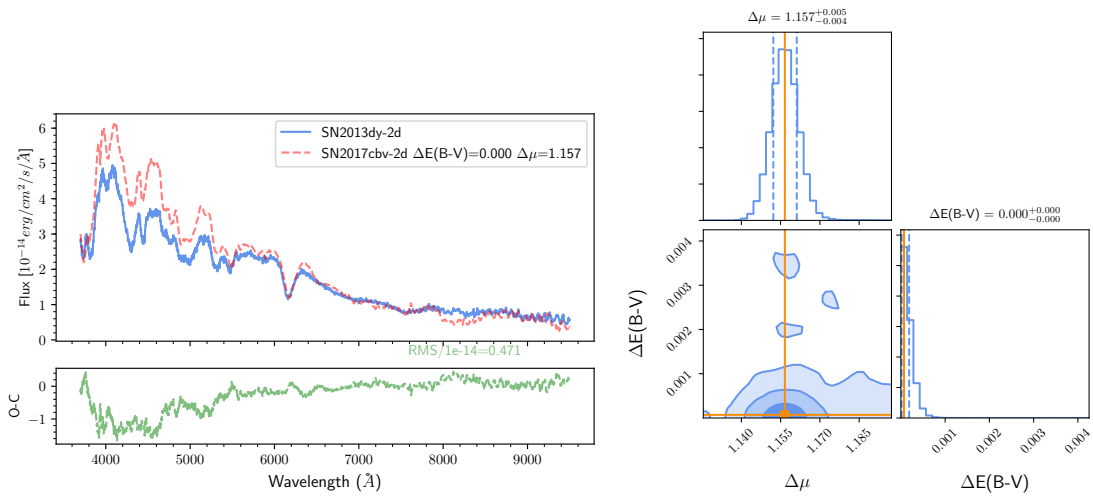


**Figure 4.** Left: Comparison of early time spectra of SN 2013dy and SN 2017cbv at -2 days before maximum light. Right: 1 $\sigma$ , 2 $\sigma$ , 3 $\sigma$  contours for this epoch.

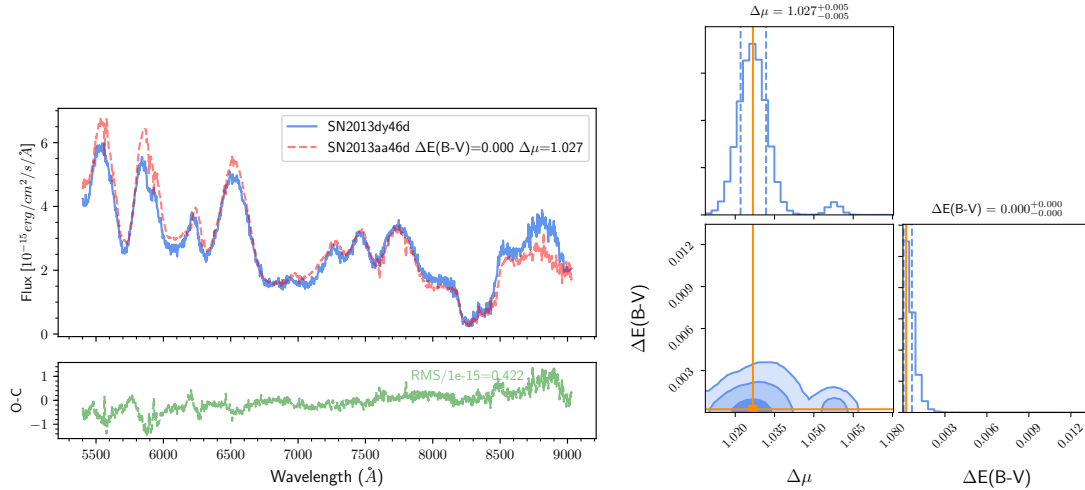


**Figure 5.** Left: Comparison of the spectra of SN 2013dy with SN 2013aa at 46 days past maximum light. Right: As above but for the 46 days phase.

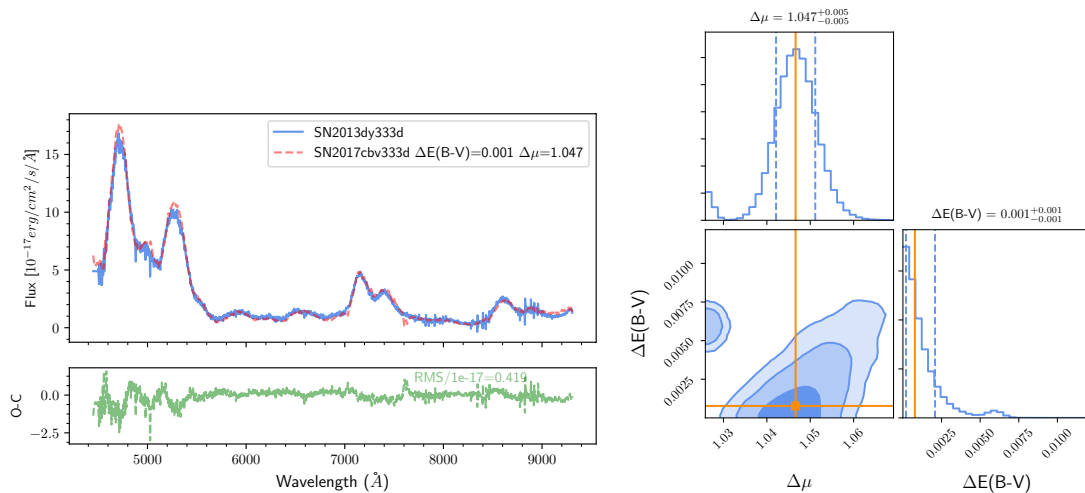


**Figure 6.** Left: Comparison of the spectrum of SN 2013dy and SN 2017cbv from late time spectra at 333 days. Right: Contours for the 333 days phase.

We see at early phase (2 days before maximum) (Figure 4) that SN 2013dy has a less steep spectrum (redder) than SN 2017cbv (and SN 2013aa). This is not due to reddening (as can be seen in later phases) but to an intrinsic slightly different effective temperature of the spectrum. The spectral features are, though, equal between SN 2013dy and its twins at early phases. One might consider that this difference can be explained by an external factor, as there is an early blue excess both in spectra and the light curve in SN 2017cbv. It has been pointed out to the presence of a companion and to an explosion from a double detonation initiated at the surface of the star for this supernova. In the case of SN 2013aa, early data are missing, so it is not possible to check whether there might have been indirect evidence for a companion. But SN 2013aa is identical to SN 2017cbv, so it might have arisen in a similar context.

From our purpose of distance determination, we exclude the earliest spectrum of SN 2013dy in our joint estimate of the distance of SN 2013dy, as there is a circumstantial factor only affecting the earliest epoch. The spectrum of SN 2013dy achieves just a few days later an amazing similarity to those of SN 2017cbv and SN 2013aa that last until the nebular phase. We obtain the derived distance to SN 2013dy from its comparison with phase 46 (Figure 5) and 333 days past maximum (Figure 6). The combined posterior distributions can be seen in Figure 7. The results on the distance are given in Table 4. One might note that  $\Delta E(B - V) = 0.0 \pm 0.000$ . The Pearson correlation coefficient  $r$  of the variables  $\Delta\mu$  and  $\Delta E(B - V)$  for the 46 phase sample = -0.025, and for the 333 phase = 0.188, thus is very low. This might be explained by the fact that we are moving around a  $\Delta E(B - V)$  very low. SN 2013dy has a similar total  $E(B - V)$  than its twins SN 2017cbv/SN 2013aa, and a reddening of  $E(B - V) = 0.01$  for SN 2013dy would arise in the host galaxy ( $E(B - V)_{MW}$  is 0.14 for SN 2013dy).

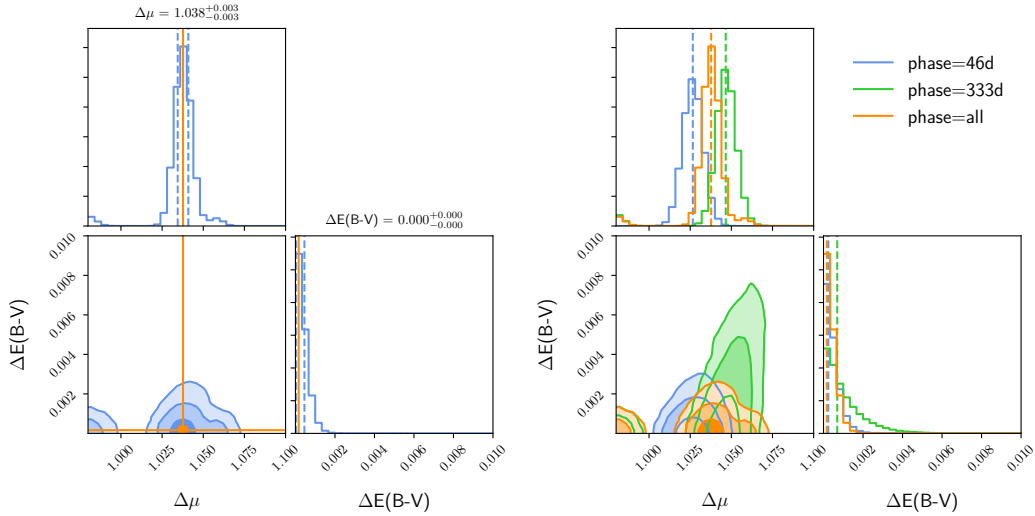


**Figure 7.** As in Figure 3. Left: Final values favored by the joint phases both 46 days after maximum and 333 days after maximum of SN 2013dy with its twins. Right: Results for each phase and the joint phases.

#### 4. THE DISTANCE TO NGC 2525

In this Section we proceed to use twin SNe Ia of other type. In particular, we are interested in the 2011fe-like group. SN 2018gv in NGC 2525 belongs to it. This allows us to determine the distance to this galaxy, for which only old, rather unrealistic Tully–Fisher distance measurements, plus a Cepheid measurement with substantial uncertainty are currently available.



**Table 4.** The distance to NGC 7250

| SN                                 | Host     | $\mu$  | Error in $\mu$ | Source                         |
|------------------------------------|----------|--------|----------------|--------------------------------|
| 2013dy                             | NGC 7250 | 31.518 | 0.003 + 0.1*   | This work                      |
| 2013dy                             | NGC 7250 | 31.628 | 0.125          | Riess et al. (2022) (Cepheids) |
| <b>Previous step in the ladder</b> |          |        |                |                                |
| 2017cbv                            | NGC 5643 | 30.480 | 0.1            | Hoyt et al. (2021)             |
| 2013aa                             | NGC 5643 | 30.480 | 0.1            | Hoyt et al. (2021)             |

\*Error in the distance to NGC 5643 of 0.1

is twice the currently estimated error.

See section about NGC 5643.

We will now use the spectral twins method to estimate the distance to NGC 2525 through the comparison between SN 2011fe and SN 2018gv from early until nebular phases.

#### 4.1. SN 2011fe in M101 as a reference

SN 2011fe was discovered, in the nearby spiral galaxy M101, in its very early phase and it was classified as a normal SN Ia (Nugent et al. 2011). It appears to have been discovered within a few hours after the explosion and this helped to put constraints on the progenitor system of the explosion (Nugent et al. 2011; Bloom et al. 2012). The pre-explosion Hubble Space Telescope image of the SN 2011fe location ruled out luminous red giants and almost all helium stars as the mass-donor companion of the exploding WD (Li et al. 2011). In addition, the early-time photometry of SN 2011fe (Bloom et al. 2012) set a limit to the initial radius of the primary star,  $R_p \leq 0.02R_\odot$ , as well as a limit to the size of the companion star,  $R_c \leq 0.1R_\odot$ . Tucker & Shappee (2023) have reported imaging follow-up of SN 2011fe during 11.5 yrs after discovery, that setting strong constraints to a possible single-degenerate progenitor systems. This result appears consistent with the lack of interaction with a non-degenerate companion in the Swift/UV light curves (Brown et al. 2012). The limits on post-impact donors by Tucker & Shappee (2023), together with constraints from pre-explosion imaging, early-time radio and X-ray observations, and nebular-phase spectroscopy, essentially rule out all formation channels for SN 2011fe invoking a non-degenerate donor star. This favours a double-degenerate progenitor for SN 2011fe.

At maximum light, the color was  $(B_{max} - V_{max}) = -0.07 \pm 0.02$  mag. The value of  $(B_{max} - V_{max})$  being  $-0.12$  mag in normal SNe Ia, this might mean that there is, in fact, some host galaxy extinction. With the removal of the Galactic component,  $E(B-V)_{MW} = 0.008$  mag (Schlafly & Finkbeiner 2011), Pereira et al. (2013) estimated such reddening as  $E(B - V)_{host} = 0.026 \pm 0.045$  mag, by using the Lira relationship of the colors in the postmaximum phase, in close agreement with the  $0.032 \pm 0.045$

mag obtained by Zhang et al. (2016). Tammann & Reindl (2011) obtained  $E(B-V)_{host} = 0.030 \pm 0.060$  mag from the B–V at the maximum of the light curves. The application of CMAGIC to SN 2011fe by Yang et al. (2020) gives a host galaxy extinction compatible with zero,  $E(B - V)_{host} = 0.0 \pm 0.027$  mag. Patat et al. (2013) studied, from multi-epoch high resolution spectroscopy of SN 2011fe, the reddening based on the absorption systems of Ca II and Na I towards the supernova. They inferred a host galaxy reddening from the equivalent width (EW) of Na I of  $E(B-V) = 0.014$  mag and they derive a Galactic reddening of  $E(B-V)_{MW} = 0.01$  mag (similar to that from Schlafly & Finkbeiner 2011). So, there is a total  $E(B-V) = 0.024$  mag from this last reference. We adopt such value as a most accurate guess, though the absolute value is not something needed for the application of the method. The reddening relative to its twin will be determined by the MCMC.

Concerning the luminosity decline parameter of SN 2011fe, Burns (2023, private communication) measured a  $\Delta m_{15}(B) = 1.07 \pm 0.006$  mag. The basic data for SN 2011fe are given in Table 5.

The derived Fe abundance in the outermost layers of the ejecta is consistent with the metallicity at the SN site in M101 ( $\sim 0.5 Z_{\odot}$ : Mazzali et al. 2015). This produces differences in the spectrum as compared with the W7 model, which has solar metallicity, with higher UV flux and affecting as well the blue spectrum at early phases. At post-maximum phases, save differences in the UV part of the spectrum, the rest of the wavelengths converge to a model based on solar metallicity such as W7. This makes twin pairing with the SN 2011fe-like SNe to be better in the optical and improving after maximum, when the photosphere has receded to the SN core. Several modeling approaches give, for SN 2011fe, an amount of  $^{56}\text{Ni}$  of  $0.5 M_{\odot}$  synthesized in the explosion. Pereira et al. (2013), from the bolometric light curve of the supernova obtain  $0.53 \pm 0.11 M_{\odot}$  of  $^{56}\text{Ni}$ . Zhang et al (2016), using as well the bolometric light curve, estimate around  $\sim 0.57 M_{\odot}$  of  $^{56}\text{Ni}$ . Mazzali et al. (2015) derived a mass of  $^{56}\text{Ni} \sim 0.47 \pm 0.05 M_{\odot}$  and a stable iron mass of  $\sim 0.23 \pm 0.03 M_{\odot}$  for SN 2011fe, based on modeling of the nebular spectra. A centrally ignited SN Ia in a Chandrasekhar-mass model similar to W7 (with production of a slightly lower mass of  $^{56}\text{Ni}$ ) seems to agree with the chemistry of this SN.

Since SN 2011fe turns to be a kind of “template” for a class of normal SNe Ia, this nearby supernova teaches us the level of  $^{56}\text{Ni}$  for that class.

A distance to M101 (the host galaxy of SN 2011fe) as that provided by the TRGB method is also in good agreement with the observed flux of the SN. Here, however, we basically deal with the difference of distances between SN 2011fe and SN 2018gv, although SN 2011fe being the anchor (the previous step of reference in the distance ladder) here, its distance enters in the final result.

**Table 5.** SN 2011fe and SN 2018gv

|  |              |                  |
|--|--------------|------------------|
| <b>SN 2011fe</b>                               |              |                  |
| RA, DEC <sup>a</sup>                           | 14:03:05.810 | +54:16:25.39     |
| Discovery date <sup>a</sup>                    | ...          | 2011-08-24       |
| Phase (referred to maximum light) <sup>b</sup> | ...          | -20 days         |
| Redshift <sup>c</sup>                          | ...          | 0.0012           |
| E(B-V) <sub>MW</sub> <sup>d</sup>              | ...          | 0.008 mag        |
| $m_B^{max}$ <sup>e</sup>                       | ...          | 9.983±0.015 mag  |
| $\Delta m(B)_{15}$ <sup>e</sup>                | ...          | 1.07±0.06        |
| Stretch factor $s_{BV}^D$ <sup>b</sup>         | ...          | 0.919±0.004      |
| Phases of the spectra used                     | ...          | 9, 289, 344 days |
| <b>SN 2018gv</b>                               |              |                  |
| RA, DEC <sup>f</sup>                           | 08:05:34.580 | -11:26:16.87     |
| Discovery date <sup>g</sup>                    | ...          | 2018-01-15       |
| Phase (referred to maximum light) <sup>f</sup> | ...          | -16 days         |
| Redshift <sup>f</sup>                          | ...          | 0.0053           |
| E(B-V) <sub>MW</sub> <sup>d</sup>              | ...          | 0.051 mag        |
| $m_B^{max}$ <sup>e</sup>                       | ...          | 12.8±0.015 mag   |
| $\Delta m(B)_{15}$ <sup>f</sup>                | ...          | 0.983± 0.15      |
| Stretch factor $s_{BV}^D$ <sup>b</sup>         | ...          | 0.937±0.031      |
| Phases of the spectra used                     | ...          | 9, 289, 344 days |

<sup>a</sup>Waagen (2011).<sup>b</sup>Richmond & Smith (2012)<sup>c</sup>Cenko et al. (2011)<sup>d</sup>Schlafly & Finkbeiner (2011).<sup>e</sup>Burns (private communication, (2023).<sup>f</sup>Yang et al. 2020.<sup>g</sup>Itagaki (2018).

#### 4.2. 2018gv

SN 2018 gv is a SN 2011fe-like supernova. The explosion was fairly symmetric and the spectra were similar all along the different phases. The supernova was discovered on 2018-01-15 by K. Itagaki in the outskirts of the host galaxy NGC 2525 (Itagaki 2018), a barred spiral galaxy at  $z = 0.00527$  (de Vaucouleurs et al. 1991).

The Galactic reddening in the direction of SN 2018gv is  $E(B-V)_{MW} = 0.051$  mag, according to the extinction map by Schlafly & Finkbeiner (2011). It is appreciably higher than that of SN 2011fe. The host galaxy reddening should be very low, given the position of SN 2018gv in the outskirts of its host galaxy. The test for reddening from the Lira relation gives that same amount, for the total reddening, as for just the Galactic one. The application of the CMAGIC method in Yang et al. (2020) gives a host reddening of  $E(B-V)_{host} = 0.028 \pm 0.027$  mag, thus being compatible with zero. The basic information on SN 2018gv can be found in Table 5. The early-time spectra of SN 2018gv show strong similarity in most respects with those of the normal Type Ia SN 2011fe (Yang et al. 2020). These authors demonstrate that SN 2018gv resembles SN 2011fe for the first 100 days and exhibits a low Si II velocity gradient in the days after peak brightness. The observation of low continuum polarization overlaid

by significant line polarization would be inconsistent with an asymmetric explosion. They suggest an amount of  $^{56}\text{Ni}$  of  $0.56 \pm 0.08 M_{\odot}$  from the bolometric light curve (Yang et al. 2020). Graham et al. (2022) show the even stronger late-time similarity between SN 2011fe and SN 2018gv. They fully deserve to be named “nebular twins”: at the same phases in the nebular evolution they have extremely similar spectra. For the application of our method, the likeness of the spectra of twin SNe Ia can not just consist of the fact that two nebular spectra might be, at some particular close times, similar. It should happen at exactly the same nebular stages. Being similar through the whole nebular phase indicates closely resembling Ni cores, which are the sources of the luminosity of the supernovae at those epochs.

As stated above, the two SNe Ia are very similar at early times, and that mostly persists until the nebular phase, with a few noticeable differences, however. So, for instance, the line width measurements suggest a slight difference in central density, though both densities are high enough to form stable Fe-group elements in the innermost regions of the core.

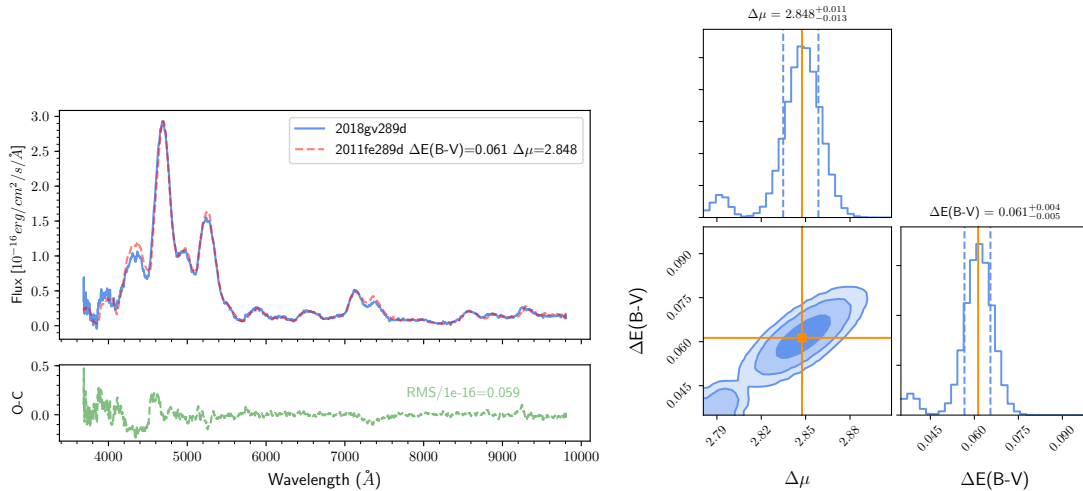


**Figure 8.** Left: Spectra of the twins SN 2011fe and SN 2018gv at exactly the same phase of 289 days past maximum light. Right: Corner plot as in previous figures but for SN 2018gv at 289 days.

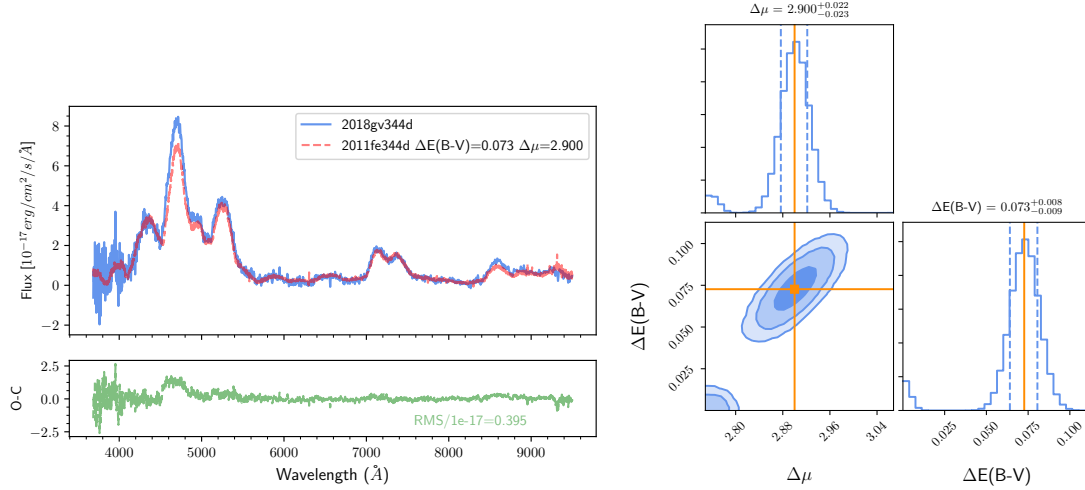


**Figure 9.** Left: Spectra of the twins SN 2011fe and SN 2018gv at exactly the same phase of 344 days past maximum light. Right: As above but for 344 days past maximum.

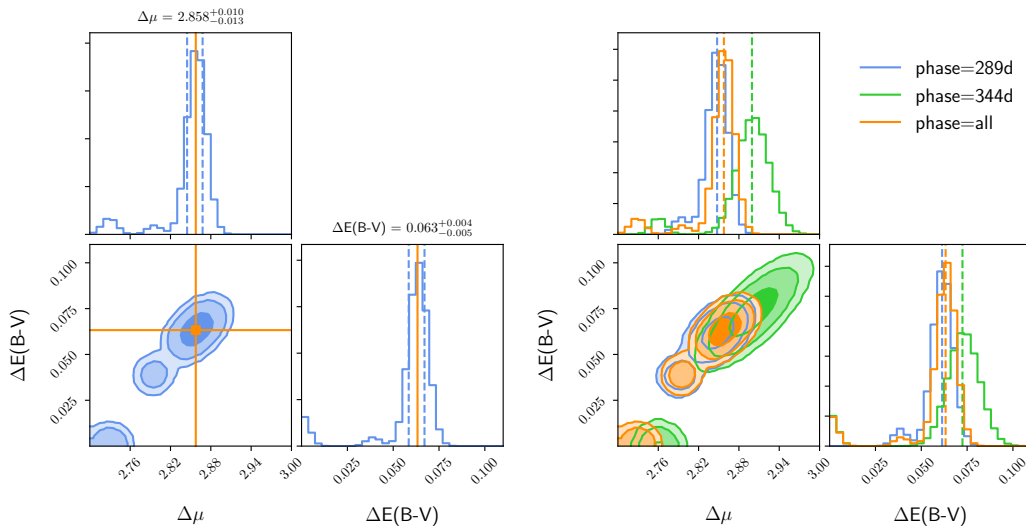


**Figure 10.** (As in Figure 3 and 7). Left: Result from the joint comparison of the two phases. Right: Individual phases and joint phases confidence regions from the comparison at 289 days after maximum and 344 days after maximum of SN 2018gv and SN 2011fe.

#### 4.3. $\Delta E(B - V)$ and distance

SN 2011fe and SN 2018gv were not heavily obscured by dust, as they occurred in the outskirts of their host galaxies. The Galactic reddening towards their direction has been measured, as stated above, by Schlafly & Finkbeiner (2011) for both SNe Ia.

To compare the spectra of the two SNe Ia, we have dereddened and deredshifted them both. SN 2011fe has been dereddened by 0.024 and SN 2018gv by 0.05 mag. The quantity  $\Delta E(B - V)$  is the amount of reddening that we would need to add to SN

2018gv to get the best fit between the spectra of the two SNe. The result,  $\Delta E(B - V)$ , indicates whether  $E(B - V)$  might be higher in SN2018gv than in SN2011fe.

The results concerning the distance are, as already stressed, a relative distance between SN 2018gv and SN 2011fe. SN 2011fe, being one of the nearest and best observed SNe Ia and a prototype “normal” SN Ia, is our first SN Ia that can work as an anchor for the extragalactic distance scale.

We search for the best match between SN2018gv and SN2011fe using only two free parameters, the reddening value difference,  $\Delta E(B - V)$ , and modulus difference  $\Delta\mu$ . We have used the similarity between the spectra of SN2011fe and SN2018gv at three different phases and we perform a fit using the likelihood function defined in [1] (Section 3).

We run again the Markov Chain Monte Carlo with 32 walkers and 10,000 steps each, implemented in EMCEE (Foreman-Mackey et al. 2013), sufficient to get a statistically significant result. In each MCMC sample our code is able to deredden the reference spectrum (that of SN 2011fe) with a given value of  $E(B - V)$  and size the parameters ( $\Delta E(B - V)$  and  $\Delta\mu$ ), relative to SN 2018gv. We adopted uniform priors on the  $\Delta D$  ( $\mathcal{U}[15, 21]$  Mpc) and reddening  $\Delta E(B - V)$  ( $\mathcal{U}[0.0, 0.8]$  mag). In Figure 8 and Figure 9, we show the posterior distributions for two different epochs and in Figure 10 the one corresponding to the combined regions. At the end, we found that the early spectrum we were going to use was not reliable as there were different reductions for the same epoch with incompatible spectral shape in the *WiSeREP* (see the above database to check this point). We should note that here the Pearson correlation coefficient  $r$  is significantly higher than for SN 2013dy, manifesting the obvious implications that a change of  $\Delta(E - V)$  has in  $\Delta\mu$  in this nearly identical spectra. As we see, the results favour  $\Delta E(B - V) = 0.063^{+0.004}_{-0.005}$  mag more in SN 2018gv than in SN 2011fe, and  $\Delta\mu = 2.858 \pm 0.013$  mag. The distance factor between SN 2018gv and SN 2011fe is 3.71:  $D_{2018gv} = 3.71 \times D_{2011fe}$ . Those are summarized in Table 6 and 8.

#### 4.4. M101

The distance to M101 has been on debate for decades. Several methods have been used to estimate the distance to M101. But finally there seems to be an agreement within a short range of discrepancy by two methods: the TRGB method and the Miras variable Period Luminosity relation. In addition, those methods are in agreement with what has been learnt about SN 2011fe in this galaxy.

At this moment, the estimates using Cepheids (*SH0ES*) differ from that obtained through TRGB and the Miras variables. But the value provided by Cepheids to the distance to this galaxy has been changing along the years. Riess et al. (2016) found

a distance modulus of  $29.135 \pm 0.045$  mag and, in Riess et al. (2022), a reanalysis of the data gave  $29.194 \pm 0.039$  mag, which place M101 at practically 7 Mpc.

Tammann & Reindl (2011) pointed out that the problem of the Cepheids in M101 is that those in the outer, metal-poor field (Kelson et al. 1996) and those in two inner, metal-rich fields (Shappee & Stanek 2011), yield discordant distances.

The TRGB distance to M101 value in Freedman et al (2019) is coming from Beaton et al. (2019). This distance modulus is  $\mu = 29.07 \pm 0.04$  (stat)  $\pm 0.05$  (sys) mag, which corresponds to a physical distance  $D = 6.51 \pm 0.12$  (stat)  $\pm 0.15$  (sys) Mpc. Huang et al. (2024) recently obtained a distance measurement to M101 using Miras variables. The value by this method is  $\mu_{M101} = 29.10 \pm 0.06$  mag in very close agreement with the TRBG distance to M101 and consistent with our expected luminosity rank of SN 2011fe (Appendix B). This is an important step for the improvement of the cosmic distance ladder.

The Mira variables value places M101 at  $6.60 \pm 0.19$  Mpc, the TRGB at  $6.51 \pm 0.27$  Mpc very much in agreement with the SN 2011fe at  $6.5 \pm 0.15$  Mpc (Appendix A).

We can say that M101 is nowadays a firm step in the cosmic ladder. It consolidates its distance in the range of  $6.4 < d < 6.7$  Mpc centered at 6.53 Mpc with a mean value for  $\mu = 29.075 \pm 0.068$  mag. The value encompasses the most recent coincident results by various methods: those mentioned above and summarized in Table 6. This convergence not only allows the calibration of many other distances for SNe Ia of the twin type that happened in M101 but also cross-checks with SNe Ia host galaxies of other twin types.

**Table 6.** Distance moduli for SN 2018gv and SN 2011fe

|        |                          |  |
|--------|--------------------------|--|
| 2018gv | $\mu = 32.067 \pm 0.10$  | Cepheids <sup>1</sup>                    |
| 2018gv | $\mu = 31.933 \pm 0.069$ | This work                                |
| 2011fe | $\mu = 29.135 \pm 0.045$ | Cepheids <sup>2</sup>                    |
| 2011fe | $\mu = 29.194 \pm 0.039$ | Cepheids <sup>1</sup>                    |
| 2011fe | $\mu = 29.07 \pm 0.09$   | Tip of the Red Giant Branch <sup>3</sup> |
| 2011fe | $\mu = 29.10 \pm 0.06$   | Mira variables <sup>4</sup>              |
| 2011fe | $\mu = 29.06 \pm 0.05$   | Appendix A                               |
| 2011fe | $\mu = 29.075 \pm 0.068$ | Obtained M101 ladder step                |

<sup>1</sup>Riess et al. (2022). <sup>2</sup> Riess et al. (2016).

<sup>3</sup>Freedman et al. (2019). <sup>4</sup> Huang et al. (2024).

We can use the convergent distance value to M101  $\mu = 29.075 \pm 0.068$  mag in our SNe Ia twins distance ladder.  $\Delta\mu$  between SN 2011fe and SN 2018gv is  $2.858 \pm 0.013$

mag in our results (see Figure 10). So, we derive  $\mu = 31.933 \pm 0.069$  mag for NGC 2525.

The determination by *SHOES* of the distance to NGC 2525 corresponds to a distance modulus of  $\mu = 32.067 \pm 0.1$  mag, which is a distance of  $25.90 \pm 1$  Mpc (Riess et al. 2022). The distance factor between SN 2018gv and SN 2011fe becomes 3.75 by Cepheids. Though it is likely that the Cepheids distance to NGC 2525 will be revised with new data from *JWST*, as has been done for other galaxies.

In our determination of the distance to NGC 2525, the distance modulus obtained corresponds to a distance of  $24.35 \pm 0.77$  Mpc when adopting the distance modulus for M101 (see Table 6). The distance factor of SN 2018gv in relation to SN 2011fe is 3.71, then. There is agreement within  $1\sigma$  with the *SHOES* value because the error in NGC 2525 with Cepheids is quite large<sup>4</sup>.

#### 4.5. NGC 5643

It might have seemed in Section 3 and Table 4 that we made an arbitrary choice in referring the distance of NGC 7250 to the NGC 5643 by Hoyt et al. (2021), and that we could have done other choice like the value provided by Cepheids in Riess et al. (2022). However, the distance values published in Riess et al. (2022) seem to have been abandoned in the case of NGC 5643 and other galaxies. There are several papers where a new Cepheid distance is given, very close to the distance by Hoyt et al. (2021), and a previous distance is quoted with the method of Cepheids, but it is not the distance in Riess et al. (2022). It is a distance very close to the TRGB value by Hoyt et al. (2021). Table 3 in Riess et al. (2024a) presents a *JWST+HST* value of the modulus to NGC 5643 of  $\mu = 30.52 \pm 0.02$  mag and a comparison value with HST (*SHOES*) of  $\mu = 30.518 \pm 0.033$  mag. The value  $\mu = 30.57 \pm 0.05$  mag from Riess et al. (2022) was the reference value of their major paper with 37 host galaxies of SNe Ia in 2022. In Riess et al. (2024a) there is no mention to this value, while it is argued that "JWST observations reject unrecognized crowding of Cepheid photometry as an explanation for the Hubble Tension at  $8\sigma$  confidence."

A compilation of the values to NGC 5643 with the Cepheids and the TRGB methods is given in Table 7.

There is another paper using TRGB by Anand et al. (2024) that suggests a new distance modulus to NGC 5643 very similar to that by Hoyt et al. (2021). Such distance is in fact  $\mu = 30.42 \pm 0.07$  mag and different from  $\mu = 30.57 \pm 0.05$  mag from Cepheids in Riess et al (2022) (*SHOES* value). The Anand et al. (2024) distance

<sup>4</sup> The TRGB distance modulus to NGC 2525 by the *SHOES* collaboration has been revised just very recently and it is now  $31.81 \pm 0.08$  mag. It is compatible with our measurement, and shorter than in Riess et al. (2022), as we expected.



**Table 7.** The distance to NGC 5643

| Galaxy   | Distance modulus (mag) | Method              | Reference                     |
|----------|------------------------|---------------------|-------------------------------|
| NGC 5643 | $30.480 \pm 0.1$       | TRGB                | Hoyt et al. (2021)            |
| NGC 5643 | $30.42 \pm 0.07$       | TRGB                | Anand et al. (2024)           |
| NGC 5643 |                        |                     | Anand et al. (2024)           |
| NGC 5643 | $30.570 \pm 0.050$     | Cepheids            | Riess et al. (2022)           |
| NGC 5643 | $30.52 \pm 0.02$       | Cepheids (JWST+HST) | Riess et al. (2024a)          |
| NGC 5643 | $30.518 \pm 0.033$     | Cepheids (HST)      | Riess et al. (2024a)          |
| NGC 5643 | $30.48 \pm 0.065$      | SN 2013aa/SN 2011fe |                               |
| NGC 5643 | $30.48 \pm 0.065$      |                     | Obtained NGC 5643 ladder step |

modulus is in fact the one found by Anand et al. (2022) reanalysing the data taken by Hoyt et al. (2021) for NGC 5643. Anand et al (2024) in their Figure 11 shows the  $\mu$  value obtained by Hoyt et al. (2021) and the one from their reanalysis in Anand et al. (2022), and they point that  $\langle TRGB - Ceph \rangle$  is very small. However, that would not be the case if the data would have been taken from Riess et al. (2022).

We have examined the distance to SN 2013aa/SN 2017cbv based in their relation towards SN 2011fe. We find that the value provided by Hoyt et al. (2021) coincided with that from the relation between SN 2013aa/SN 2017cbv SNe Ia and SN 2011fe types. There is a consistent ladder step reflecting the amount of radioactive material synthesized in the explosion of this type versus other ones like SN 2011fe (see next section). Given the coincidence in distances as shown in Table 7 with the TRGB and within the recent Cepheid values, we think that there is a good based ladder step in NGC 5643 at a  $\mu$  of  $30.48 \pm 0.065$  mag.

It is good to find convergence in some new distance values for a few galaxies between Cepheids and TRGBs, however the previous larger data set with important disagreements should be mentioned as well. Otherwise, there is a loss of credibility in the conclusions.

We note, in a previous version of the paper, that the Cepheid distance modulus for NGC 5643 of  $\mu = 30.57 \pm 0.05$  mag and for M101 of  $\mu = 29.194 \pm 0.039$  mag in Riess et al. (2022) had central larger values than those from the TRGB, despite the higher  $H_0$  around  $73 \text{ km s}^{-1} \text{ Mpc}^{-1}$  obtained by this method compared with  $69 \text{ km s}^{-1} \text{ Mpc}^{-1}$  favored by the TRGB. This could have been a fluctuation. However, the new values published in 2024 put back in agreement the distances for those two galaxies with those of the CCHP (Freedman et al. 2019) using the TRGB method.

## 5. DISCUSSION

While the use of twins has been proved to be very useful for distance determinations, pairing SNe Ia which are not true twins can lead to errors in distance estimates. A

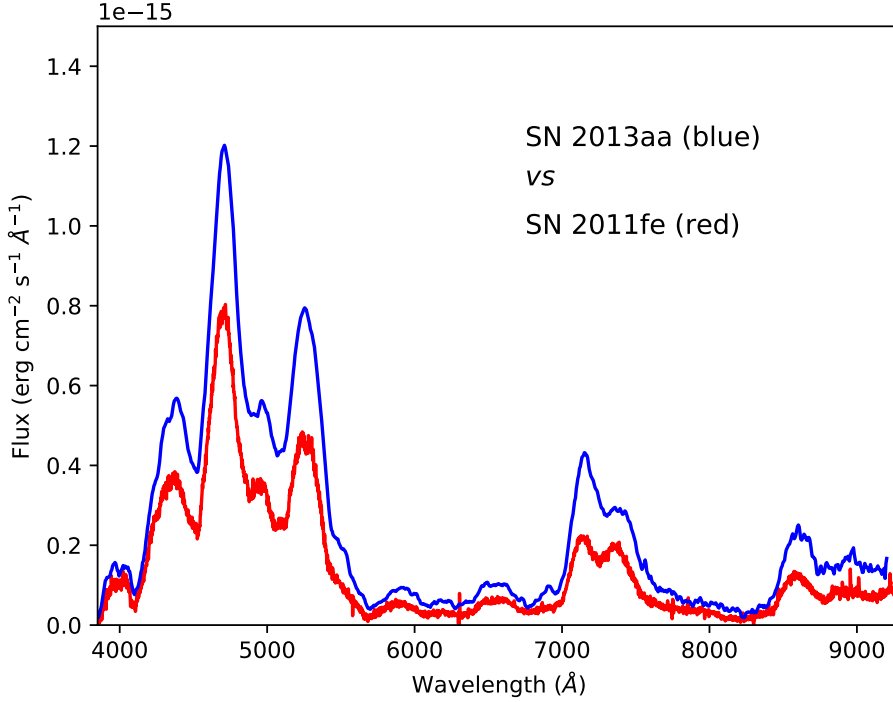


**Figure 11.** Comparison of the spectra of SN 2013aa and SN 2011fe at the same phase. The reddening of SN 2011fe has been placed at  $E(B-V) = 0.15$  to compare it with SN2013aa.

good first order guide is to explore only SNe Ia within similar stretch values  $s_{BV}$ . Then, within a similar stretch family, one can compare the spectra at various phases, as we have done here. We have looked to twins of the SN 2013aa/SN 2017cbv class, as well as to the SN 2011fe class.

How to size the difference in between SNe Ia twin classes?. If we placed 2013aa at the distance of 6.5 Mpc for SN 2011fe, we find a factor of 1.46 of difference in flux level. If we wrongly took SN 2013aa for a twin of SN 2011fe, the error in distance would be by a factor of 1.208 (see Figure 11).

There is a lack of the spectral line of stable Ni in SN 2013aa, which indicates that the WD ignited at a lower central density than in SN 2011fe there. The line due to the presence of stable Ni isotopes points to a start of the ignition at high densities, in SN 2011fe. Both SN 2011fe and SN 2018gv underwent explosive burning at a higher density than SN 2017cbv and SN 2013aa. The mismatch between them is seen at both early and late phases. In fact, SN 2013aa and SN 2017cbv synthesized about  $0.23 M_{\odot}$  more  $^{56}\text{Ni}$  than the pair SN 2011fe and SN 2018gv, as suggested by the overall higher flux. This is corroborated by previous studies (Jacobson-Galán et al. 2018) suggesting  $0.732 \pm 0.151 M_{\odot}$  of  $^{56}\text{Ni}$  in SN 2013aa. Those authors obtained such a value for  $^{56}\text{Ni}$  in SN 2013aa using a particular approach at late phases (a sort

of rate of decline of the bolometric light curves, with stretch described in Graur et al. (2018) and using as well the Arnett’s law at early phases.

It seems that the class of SN 2013aa/SN 2017cbv is well understood and if a SNIa of this kind would happen in galaxies far enough to have a measured redshift not affected by peculiar velocities, a good measurement of  $H_0$  should be possible.

### 5.1. *The whole SNe Ia calibrating sample*

By looking at the nebular spectra of the sample of SNe Ia in the calibrating samples of galaxies of TRGB (18 SNe Ia in 15 galaxies) of Freedman et al. (2019), and in the calibrating sample of 42 SNe Ia in 37 galaxy hosts of Riess et al. (2022), we have twins of SN 2011fe, as well as twins of SN 2017cbv/2013aa. There is also the class of SNe Ia with light echos, which can be close to the normal SN 2011fe or to the overluminous SN 1991T in those calibrating samples. In fact, SN 1991T had an echo. There seems to be as well a class represented by SN 2012cg with its twin SN 2009ig, which show evidence of interaction with a non-degenerate companion. The lack of strong lines of stable Ni points to ignition at a lower density than in SN 2011fe, there.

In general, in those SNe Ia lists, there is a range of SNe Ia which have synthesized different amounts of  $^{56}\text{Ni}$  (from 0.4 to 0.8  $M_\odot$ ) and have undergone thermonuclear burning at different densities. In addition, SNe Ia do have peculiarities such as evidence for an early interaction with a supernova companion, or the presence of an echo at late times.

For the first time, a long coverage of a SN Ia at the nebular phase has been obtained, from 400 days to 1000 days in the case of SN 2011fe (Tucker et al 2022). We have seen clearly how the ionization stage changes significantly along this time, for this normal SN Ia. But even from 200 to 460 days the level of ionization of  $\text{Fe}^+$  and  $\text{Fe}^{++}$  undergoes significant change.

A dense grid of nebular spectra of SNe Ia would facilitate the twins classification. The use of this database should enable comparison of spectra of different supernovae at similar dates. The use of different SNe Ia at significant different phases, as if they were at the same phase, which is nowadays often done at late times, should be avoided. It affects the evaluation of the masses of NSE nuclides synthesized in the explosion. The abundances of stable NSE nuclides are indicators of the densities at which the WDs explode and they also give clues about the mechanism involved in the explosion. But, for the present case, the overall flux of the elements from the decay of  $^{56}\text{Ni}$  synthesized in the explosion make the overall flux of the spectra at late times, therefore affecting any distance determination.

Reliable distances can be obtained by pairing the twins until the nebular phase, once proper flux calibration and choice of similar phases are done. Including the nebular

phase can prevent errors made when matching the very early phases, at which times different interactions with circumstellar material or possible heating from a companion would produce differences in the spectra.

The distance to M101 from Beaton et al. (2019) using the TRGB method is consistent with SN 2011fe having synthesized  $0.5 M_{\odot}$  of  $^{56}\text{Ni}$ , as most authors have found.

The difference between SN 2011fe and the SN 2017cbv/2013aa suggests that that NGC 5643 is at  $\mu = 30.48 \pm 0.065$  mag. The convergent value on M101 from previous section is  $\mu = 29.075 \pm 0.068$  mag and NGC 7250 is at  $\Delta d = 7.64 \pm 0.03$  Mpc from our joined twin SNe Ia spectra from NGC 5643, thus at  $31.518 \pm 0.065$  mag. The NGC 5643 value derived by the Cepheids is  $31.628 \pm 0.126$  mag from *SHOES* (Riess et al. 2022), which does not yet use *JWST* and would likely be reexamined.

We include in Table 8 the distance values using the "SNe Ia twins for life" method as well as those provided by other methods, as discussed in the main text.

**Table 8.** Moduli and distances from the present work *vs* Cepheid and TRGB moduli

| Galaxy   | $\mu$ (mag)        | D (Mpc)          | $\mu$ Cepheids (mag) <sup>1</sup> | $\mu$ TRGB (mag)              |
|----------|--------------------|------------------|-----------------------------------|-------------------------------|
| M 101    | $29.075 \pm 0.068$ | $6.53 \pm 0.20$  | $29.194 \pm 0.039$ <sup>2</sup>   | $29.08 \pm 0.04$ <sup>3</sup> |
| NGC 5643 | $30.48 \pm 0.065$  | $12.47 \pm 0.37$ | $30.570 \pm 0.050$ <sup>4</sup>   | $30.48 \pm 0.1$ <sup>5</sup>  |
| NGC 7250 | $31.518 \pm 0.065$ | $20.12 \pm 0.70$ | $31.628 \pm 0.126$                | ...                           |
| NGC 2525 | $31.933 \pm 0.069$ | $24.35 \pm 0.77$ | $32.067 \pm 0.100$                | ...                           |

<sup>1</sup>Riess et al. (2022). <sup>2</sup> $29.10 \pm 0.06$  from Mira variables (Huang et al. 2024). <sup>3</sup>Freedman et al. (2019). <sup>4</sup>Changed to  $30.52 \pm 0.02$  in Riess et al. (2024a). <sup>5</sup>Hoyt et al. (2021).

The method has been applied as well to the twins of SN 2011fe in M101 and SN 2018gv in NGC 2525. This has allowed to determine a distance of  $24.35 \pm 0.77$  Mpc to NGC 2525. The value reported by Riess et al. (2022) is  $25.90 \pm 1$  Mpc. Our result presented here is compatible with that from the Cepheids due to the large error on the distance determination. It does not align well with the extreme distance  $\sim 27$  Mpc in the upper edge of the uncertainty towards NGC 2525 obtained from the Cepheids.

The *SHOES* collaboration measurement places SN 2018gv at a relative distance factor  $\sim 3.75$  times that of SN 2011fe, while we favor a factor  $\sim 3.71$ .<sup>5</sup>

It seems clear that twins followed until the nebular phase can establish the distance ladder in the epoch of large surveys. The infrared part of the nebular spectra of SNe Ia will soon become widely available, from programs already approved for the *JWST*. The infrared will reveal further differences among SNe Ia in that part of the spectra, thus helping in the twin classification.

## 6. CONCLUSIONS

It has been proved here that comparison of twin SNe Ia can provide a robust way to establish the extragalactic distance ladder. The method has been applied to the twins in the galaxy NGC 5643: SN 2013aa and SN 2017cbv. The comparison using spectra before maximum and at the nebular phase shows that the error in the distance determination is of  $\Delta\mu \sim 0.005$  mag.

Distances obtained here for NGC 7250 and NGC 2525 are consistent with those obtained by Riess et al. (2022) given the large error bars of the distances to these galaxies by those authors. Our distances are somehow shorter and with smaller errors than those in the mentioned paper. Now, the very recently revised value published in Li et al. (2024) to NGC 2525 agrees with our suggestion made since the first version of this manuscript. The value of the distance to NGC 5643 (Hoyt et al. 2021) is in good accordance with the one derived by the SNe Ia in this paper, but not with that was presented by Riess et al. (2022). The difference of  $\mu_{Cepheids} = 30.57 \pm 0.05$  mag versus  $\mu_{TRGB} = 30.48 \pm 0.1$  mag by Hoyt et al. (2021) is larger than the usual 0.05 mag ( $\Delta\mu \sim 0.1$ ), leaving aside the errors. If one takes into account that NGC 5643 is a nearby galaxy, the difference called for a revision, as we mentioned in an earlier version of this paper. Such revision has been done in Riess et al. (2024b) with Cepheids in NGC 5643 observed with the *JWST* and a value of  $\mu = 30.52 \pm 0.02$  has been obtained providing a much better agreement between methods. We found a need of a similar revision of the Cepheids distance to NGC 7250 and NGC 2525 in the first version of this manuscript, and this revision has been made successfully. Our method has proved to find inconsistencies in the distance moduli given by Cepheids or TRGB, therefore being very useful. More distance moduli will soon see the light from the *JWST* data analysis.

In the near future, we plan to complete the check for the galaxy sample measured by Cepheids and TRGB published so far by applying our method. But we want to go to

<sup>5</sup> Very recently, new measurements of the distances to the galaxies in Table 8 have been published. They have been obtained with data from the *JWST* by Freedman et al. (2024). For the galaxy NGC 7250, they obtain using Cepheids a distance modulus of  $31.41 \pm 0.12$  mag while using TRGB they find a distance of  $31.62 \pm 0.04$  mag. So, our measurement lies in the middle, being compatible within  $1\sigma$ . This team has revised as well the distance to NGC 5643 with the new *JWST* data and they find a distance modulus of  $30.51 \pm 0.08$  mag using Cepheids and  $30.61 \pm 0.07$  mag using TRGBs. Our favored distance is within  $1\sigma$ . The *SHOES* team has, on the other hand, revised their distance to NGC 2525 using TRGBs and they find a distance modulus of  $31.81 \pm 0.80$  mag, compatible with our distance, but now with a smaller error bar and lower central value for the distance modulus, as we had suggested.

distant galaxies as a priority, as we suspect that a major difference in the  $H_0$  value from Cepheids and from TRGBs might arise from the different procedure followed to link the local SNe Ia sample with that one in the Hubble flow.

The way to evade the problem is to obtain  $H_0$  using SNe Ia twins in galaxies of the Coma cluster or any galaxy at  $z \sim 0.02\text{--}0.03$ , already in the Hubble flow and compare them with their local SNe Ia twins. We would like to extend the method of the twin distance determinations to SNe Ia in the Hubble flow observing spectra not only near maximum, but also well into the epochs where SNe Ia show the diversity of the inner core, specially the Fe-peak elements and  $^{56}\text{Ni}$ -rich innermost layers. That should be achievable with the *JWST* or the *ELT*.

The authors would like to thank Melissa Graham and Chris Burns for generously providing spectra used in the present paper. This work has made use as well of spectra from the *Weizmann Interactive Supernova data REPOSITORY (WISEREP)*. Gaia DR3 photometry was used in the calibration of SN 2018gv/Gaia18bat data. We acknowledge *ESA Gaia, DPAC and the Photometric Science Alerts Team* (<http://gsaweb.ast.cam.ac.uk/alerts>). PR-L would like to thank Michael Weiler and Josep Manel Carrasco from the Gaia-ICCUB team for their help in crosschecking the calibration of the spectra of SN 2018gv at late phases. PR-L also acknowledges support from grant PID2021-123528NB-I00, from the the Spanish Ministry of Science and Innovation (MICINN). JIGH acknowledges financial support from MICINN grant PID2020-117493GB-I00.

## REFERENCES

- Anand, G.A., Riess, A.G., Yuan, W., et al. 2024, ApJ, 996, 89
- Beaton, R.L., Seibert, M., Hatt, D., et al. 2019, ApJ, 885, 141
- Bernal, J.L., Verde, L., & Riess, A.G. 2016, JCAP, 10, 019
- Blakeslee, J.P., Jensen, J.B., Ma, C.-P., Milne, P.A., & Greene, J.E. 2021, ApJ, 911, 65
- Bloom, J.S., Kasen, D., Sen, K.J., et al. 2012, ApJL, 144, L17
- Boone, K., Fakhouri, H., Aldering, G.A., et al. 2016, AAS Meeting, 227, 237.10, NASA ADS: 2016AAS...22723710B
- Boone, K., Aldering, G., Antilogus, P., et al. 2021, ApJ, 912, 71
- Branch, D., Dang, L.C., Hall, N., et al. 2006, PASP, 118, 560

- Brown, P.J., Dawson, K.S., Harris, D.W., et al. 2012, *ApJ*, 749, 18
- Burns, C.R., Stritzinger, M., Phillips, M.M., et al. 2014, *ApJ*, 789, 32
- Burns, C.R., Ashall, C., Contreras, C., et al. 2020, *ApJ*, 895, 118
- Casper, C., Zheng, W., Li, W., et al. 2013, *CBET*, 3588, 1, NASA ADS: 2013CBET.3588....1C
- Cenko, S.B., Thomas, R.C., Nugent, P.E., et al. 2011, *ATel*, 3583, 1
- de Vaucouleurs, G., de Vaucouleurs, A., Corwin, H.G. et al. 1991, *Third Reference Catalogue of Bright Galaxies, Vol. 1* (Springer, New York), ISBN 3-540-97552-7; 0-387-97552-7
- Di Valentino, E., Melchiorri, A., & Silk, J. 2021, *ApJL*, 908, L9
- Efstathiou, G., Rosenberg, E., & Poulin, V. 2024, *Phys. Rev. Lett.*, 132, 221002
- Fakhouri, H.K., Boone, K., Aldering, G., et al. 2015, *ApJ*, 815, 58
- Foreman-Mackey, D., Hoog, D.W., Lang, D., & Goodman, J. 2013, *PASP*, 125, 300
- Freedman, W.L., Madore, B.F., Hatt, D., et al. 2019, *ApJ*, 882, 34
- Freedman, W.L., & Madore, B.F. 2023, *JCAP*, 11, 050
- Freedman, W.L., Madore, B.F., Jiang, I.S., Hoyt, T.J., Lee, A.J., & Owens, K.A. 2024, arXiv:2408.06153
- Gelman, A., Carlin, J.B., Stern, H.S., Dunson, D.B., Vehtari, A., & Rubin, D.B. 2014, *Bayesian Data Analysis*, by A. Gelman et al. Third edition, Boca Raton, FL, Chapman & Hall, ISBN 13-9781-43984-0955, NASA ADS: 2014bda..book.....G
- Goodman, J., & Weare, J. 2010, *Communications in Applied Mathematics and Computational Science*, 5, 65, DOI: 10.2140/camcos.2010.5.65
- Graham, M.L., Kennedy, T.D., Kumar, S., et al. 2022, *MNRAS*, 511, 3682
- Graur, Or, Zurek, D.R., Cara, M., et al. 2018, *ApJ*, 866, 10
- Guy, J., Astier, P., Nobili, S., Regnault, N., & Pain, R. 2005, *A&A*, 443, 781
- Hoyt, T., Beaton, R.L., Freedman, W.L., et al. 2021, *ApJ*, 915, 34
- Hamuy, M., Phillips, M.M., Maza, J. et al. 1995, *AJ*, 109, 1

- Hamuy, M., Cartier, R., Contreras, C., & Suntzeff, N.B. 2021, MNRAS, 500, 1095
- Huang, C.D., Yuan, W., Riess, A.G., et al. 2024, ApJ, 963, 83
- Itagaki, K. 2018, TNSTR, 57, 1
- Jacobson-Galan, V.W., Dimitriadis, G., Foley, R.J., & Kirpatrick, C.D. 2018, ApJ, 857, 88
- Jha, S., Riess, A.G., & Kirshner, R.P. 2007, ApJ, 659, 122
- Kelson, D.D., Illingworth, G.D., Freedman, W.L., et al. 1996, ApJ, 463, 26
- Kenworthy, W.D., Riess, A.G., Scolnic, D., et al. 2022, ApJ, 935, 83
- Khetan, N., Izzo, L., Branchesi, M., et al. 2021, A&A, 647, A72
- Li, S., Anand, G.S., Riess, A.G., et al. 2024, arXiv:2408.0006
- Li, W., Bloom, J.S., Podsiadlowski, P., et al. 2011, Natur, 480, 348
- Madore, B.F., & Freedman, W.L. 2024, ApJ, 961, 166
- Mazzali, P.A., Sullivan, M., Filippenko, A.V., et al. 2015, MNRAS, 450, 2631
- Morrell, N., Phillips, M.M., Folatelli, G., et al. 2024, ApJ, 967, 20
- Murakami, Y.S., Riess, A.G., Stahl, B.E., et al. 2023, JCAP, 11, 046
- Nomoto, K., Thielemann, F.-K., & Yokoi, K. 1984, ApJ, 286, 644
- Nugent, P., Phillips, M.M., Baron, E., Branch, D., & Hauschildt, P. 1995, ApJL, 455, L147
- Nugent, P.E., Sullivan, M., Cenko, S.B., et al. 2011, Natur, 480, 344
- Pan, Y.C., Foley, R.J., Kromer, M., et al. 2015, MNRAS, 452, 4307
- Parrent, J.T., Sand, D., Valento, M., Graham, D.A., & Howell, D.A. 2013, ATel, 4817, 1
- Patat, F., Cordiner, M. A., Cox, N. L. J., et al. 2013, A&A, 549, A62
- Pereira, R., Thomas, R.C., Aldering, G., et al. 2013, A&A, 554, A27
- Peterson, E.R., D’Arcy Kenworthy, W., Scolnic, D., et al. 2022, ApJ, 938, 112



- Perlmutter, S., Aldering, G., Goldhaber, G., et al. 1999, *ApJ*, 517, 565
- Phillips, M.M. 1993, *ApJL*, 413, L105
- Phillips, M.M., Lira, P., Suntzeff, N.B., et al. 1999, *AJ*, 118, 1766
- Planck Collaboration 2020, *A&A*, 641, A6
- Richmond, M.W., & Smith, H.A. 2012, *JAVSO*, 40, 872
- Riess, A.G., Press, W.H., & Kirshner, R.P. 1996, *ApJ*, 473, 88
- Riess, A.G., Filippenko, A.V., Challis, P., et al. 1998, *AJ*, 116, 1009
- Riess, A.G., Macri, L.M., Hoffmann, S.L., et al. 2016, *ApJ*, 826, 56
- Riess, A.G., Yuan, W., Macri, L.M., et al. 2022, *ApJ*, 934, L7
- Riess, A.G., Anand, G.S., Yuan, W., et al. 2024a, *ApJL*, 962, L17
- Riess, A.G., Scolnic, D., Anand, G.S., et al. 2024b, *arXiv:2408.11770*
- Rubin, D., Aldering, G., Betoule, M., et al. 2023, *arXiv:2311.12098*
- Ruiz-Lapuente, P., & Lucy, L.B., 1992 *ApJ*, 400, 127
- Ruiz-Lapuente, P. 1996, *ApJ*, 465, L83
- Shappee, B.J., & Stanek, K.Z. 2011, *ApJ*, 733, 124
- Schlafly, E.F., & Finkbeiner, D.P. 2011, *ApJ*, 737, 103
- Schneider, S.E., Thuan, T.X., Mangum, J.G., & Miller, J. 1992, *ApJS*, 81, 5
- Scolnic, D., Brout, D., Carr, A., et al. 2022, *ApJ*, 938, 113
- Shingles, L.J., Sim, S.A., Kromer, M., et al. 2020, *MNRAS*, 492, 2029
- Shingles, L.J., Flors, A., Sim, S.A., et al. 2022, *MNRAS*, 512, 6150
- Stritzinger, M., Hamuy, M., Suntzeff, N.B., et al. 2002, *AJ*, 124, 2100
- Suntzeff, N.B., Hamuy, M., Martin, G., Goomez, A., & Gonzalez, R. 1988, *AJ*, 96, 1864
- Tammann, G.A., & Reindl, B. 2011, *arXiv:1112.0439*
- Tartaglia, R., Sand, D., Wyatt, S., et al. 2017, 10158, *NASA ADS: ATel10158....1T*

Tucker, M.A., Shappee, B.J., Kochanek, C.S., et al. 2022, MNRAS, 517, 4119

Tucker, M.A., & Shappee, B.J. 2024, ApJ, 962, 74

Waagen, E.O. 2011, AAN, 446, 1

Waagen, E.O. 2013, AAN, 479, 1

Wilk, K.D., Hiller, D.J., & Dessart, L. 2018, MNRAS, 474, 3187

Yang, Y., Hoefflich, P., Baade, D., et al. 2020, ApJ, 902, 46

Zhai, Q., Zhang, J.-J., Wang, X.F., et al. 2016, AJ, 151, 125

Zhang, K., Wang, X., Zhang, J., et al. 2016, ApJ, 820, 677

Zheng, W., Silverman, J.M., Filippenko, A.V., et al. 2013, ApJL, 788, L15

## APPENDIX

### Appendix A. Signatures for identifying twins. The example of SN 2017cbv/2013aa and SN 2011fe

We have stated that twins belong to a similar stretch class and, moreover, they only differ in colours by around 0.04 mag. The shape of the pseudo-continuum should be similar, therefore. We address this comparison in the first place. One can also expect that the spectral features in twin SNe Ia will be very similar. This can be quantified by the usual ratios that characterize the sample of SNe Ia. We refer here, in the second place, to the work on pseudo-equivalent widths among SNe Ia. In the third place, we will refer to the ratio of the two lines of Si II at  $\lambda$  5972 Å and  $\lambda$  6355 Å.

#### I. Pseudo-continuum.

In the early phases the amount of  $^{56}\text{Ni}$  synthesized in the SNIa explosion determines to have a hotter or cooler photosphere. A SN Ia with more  $^{56}\text{Ni}$  will show a higher effective temperature ( $T_{\text{eff}}$ ) of the pseudo-continuum.

We have compared the spectra of SN 2017cbv/SN2013aa at -2d with that of SN 2011fe and it shows that the shape of the pseudo-continuum is that of a Planck function with  $T_{\text{eff}}$  of 25,000 K while for the same phase in SN 2011fe the shape provides 23,000 K, thus 2000 K lower (see Figure 12). We have also compared the spectrum of SN 2017cbv at 12 days past maximum and the difference is also of 2000K. The spectrum of SN 2017cbv shows a pseudo-continuum of 21,000 K while the spectrum of SN 2011fe fits with a  $T_{\text{eff}}$  of 19,000 K (see Figure 13).

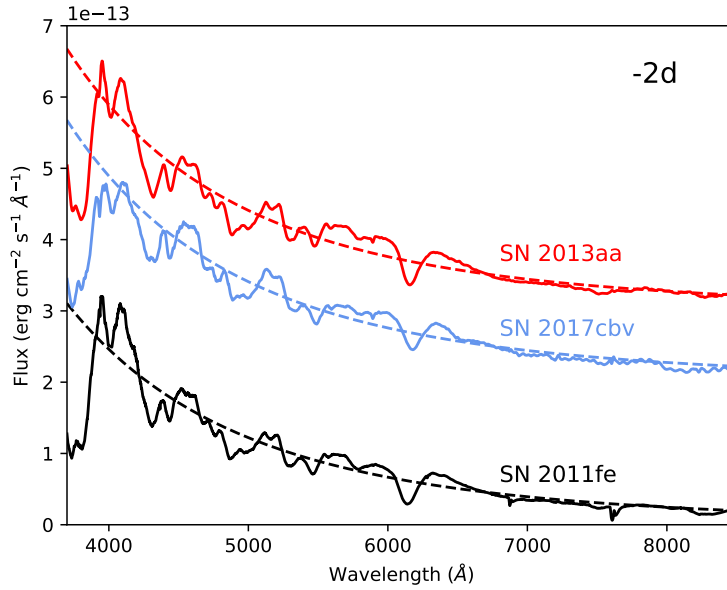


**Figure 12.** Comparison of SN 2017cbv/SN2013aa with SN2011fe at 2 days before maximum. The  $T_{\text{eff}}$  of the photosphere of SN 2017cbv/2013aa is 2000 K higher than in SN 2011fe.

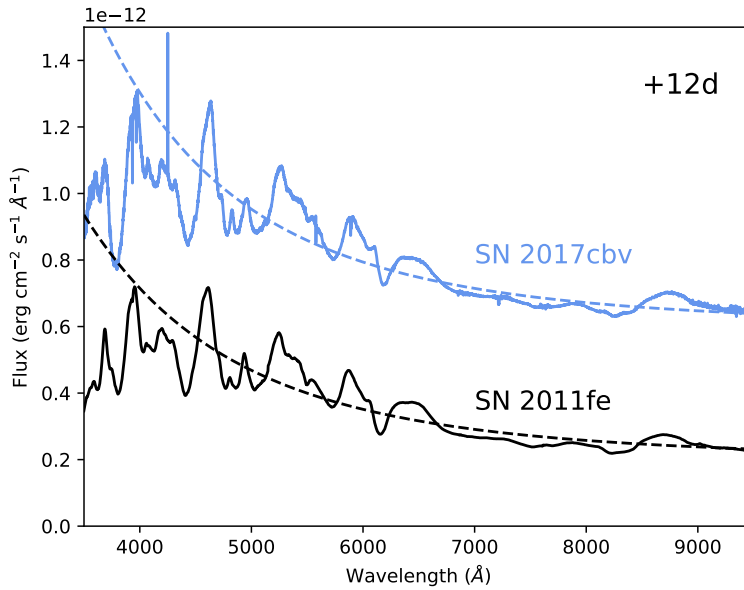


**Figure 13.** Comparison of SN 2017cbv/SN2013aa with SN2011fe at 12 days past maximum. The  $T_{\text{eff}}$  of the photosphere of SN 2017cbv is 2000 K higher than in SN 2011fe.

## II. pWs

The pseudo-equivalent widths of different lines near maximum of SNe Ia are the basis of the Branch classification of SNe Ia, which informs about the inner distributions

of elements in the velocity space of the supernova ejecta. The classes are "shallow silicon" (SS), "core normal" (CN), "broad line (BL) and "cool line" (CL) (Branch et al, 2006). SN 2017cbv and SN 2013aa belong to the "core normal" class, as SN 2011fe. Burns et al. (2020) measure the pseudo-equivalent widths of SN 2017cbv and SN 2013aa and, in their Figure 8, pWs of  $\lambda$  5972 Å versus  $\lambda$  6355 Å reveal that both SNe Ia are very close in the core-normal region of the Branch diagram. We have measured the pWs of those lines and found that they are as in Burns et al. (2020). SN 2011fe is also a CN SNe Ia, but shows different pWs than the class of SN 2017cbv and SN 2013aa.

The depths of the various lines is a measure of their similarity as SNe Ia explosions and this is correlated with the stretch/rate of decline  $s_{BV}/\Delta m_{15}$  (see, for the latest on this, Morrell et al. 2024).

The diagnostics is clearer for the SNe Ia spectra which do not come with blends from other lines. This is the case for CaII H & K (pW1), and the double S II "W" feature at 5400 Å which is a clear blend dominated by S II (pW5). It is also the case for the Si II  $\lambda$  5972 Å line (pW6) and the Si II  $\lambda$  6355 Å (pW7). We can see the difference of the values between SN 2017cbv/2013aa and SN 2011fe (see Table 9). The trend between the Si II pWs of the mentioned lines and the rate of decline  $s_{BV}$  or  $m(B)_{15}$  is well illustrated in Morrell et al. (2024). We confirm such correlation.

**Table 9.** Photometric and spectroscopic characteristics of SNe Ia

| Supernova  | $\Delta m_{15}$ (B)<br>[mag] | $s_{BV}^D$  | pW1 (Ca II H&K)<br>[Å] | pW5 (S II W)<br>[Å] | pW6 (Si II 5972)<br>[Å] | pW7 (Si II 6355)<br>[Å] |
|------------|------------------------------|-------------|------------------------|---------------------|-------------------------|-------------------------|
| SN 2011fe  | 1.07±0.06                    | 0.919±0.004 | 111±1                  | 74±1                | 16.0±0.5                | 98±1                    |
| SN 2013aa  | 0.96±0.01                    | 1.11±0.02   | 74±1                   | 67±1                | 10.0±0.5                | 84±1                    |
| SN 2017cbv | 0.96±0.02                    | 1.11±0.03   | 64±1                   | 69±1                | 10.0±0.5                | 76±1                    |

### III. Si II ratio $\mathfrak{R}_{Si}$

**Table 10.** Si II  $\lambda\lambda$ 5972/6355 ratios

| Supernova  | $\mathfrak{R}_{Si}$ |
|------------|---------------------|
| SN 2011fe  | 0.23±0.05           |
| SN 2013aa  | 0.10±0.05           |
| SN 2017cbv | 0.13±0.05           |

The ratio of the two Si II lines, Si II  $\lambda$  6355 Å and Si II  $\lambda$  5972 Å defines the  $\mathfrak{R}_{SiII}$  parameter as introduced by Nugent et al. (1995). According to Nugent et al (1995),

the Si II lines interact with line blanketing from Fe III and Co III at pre–maximum when the temperature is high and Fe and Co are substantially present in the outer layers. This effect washes out the  $\lambda$  5972 Å line and makes  $\mathcal{R}_{Si}$  lower than for SNe Ia with lower temperatures near and in the pre–maximum. Here we show how in SN 2017cbv and SN 2013aa  $\mathcal{R}_{Si}$  is lower than for SN 2011fe (see Table 10). We underlined in the first subsection of this Appendix A how the effective temperatures of SN 2017cbv and SN 2013aa are typically 2000K higher than in SN 2011fe at various phases. So, this is consistent with the different  $\mathcal{R}_{SiII}$ .

## B. Theoretical anchor for SN 2011fe in M101

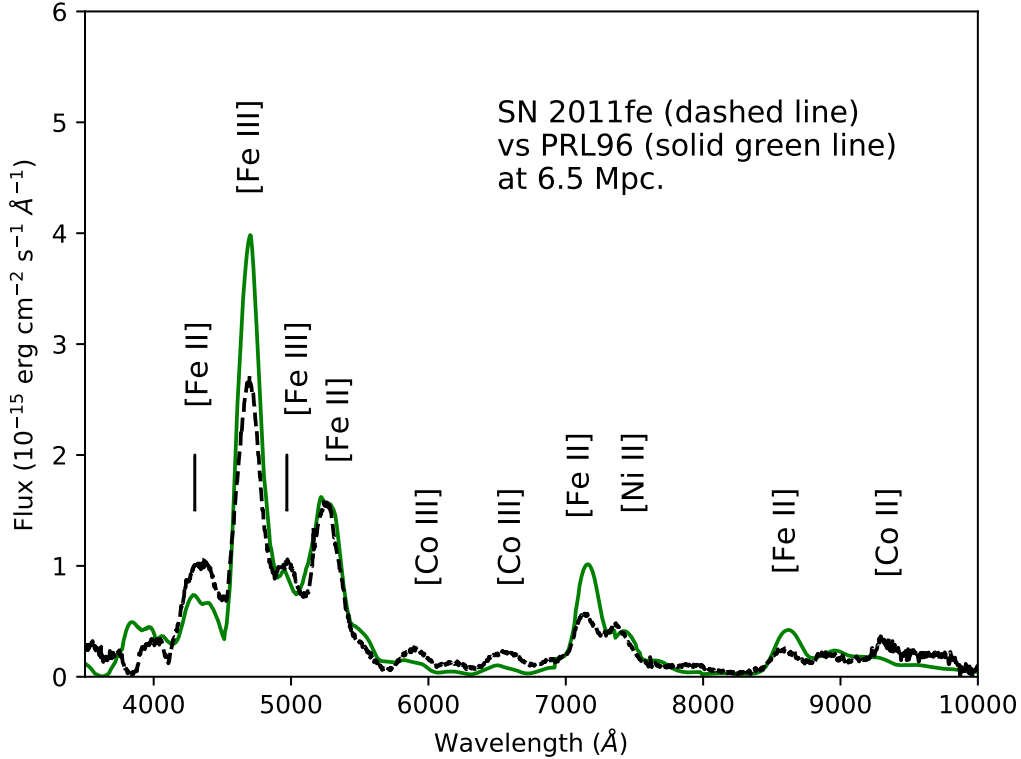


**Figure 14.** A distance of 6.5 Mpc seems compatible with the late time spectrum of SN 2011fe. Here a comparison is made with a theoretical spectrum with a  $^{56}\text{Ni}$  mass of  $0.5 M_{\odot}$  of the W7 class obtained with the code explained in Ruiz–Lapuente (1996).

At late phases, the population of the energy levels of the ions present in the supernova ejecta is out of LTE because the density of the electrons responsible for collisionally exciting the lines is lower than the critical density for the corresponding transitions. Forbidden emission can be exploited here, since such emission from iron ions (especially  $\text{Fe}^+$ ) trace very well the electron density ( $n_e$ ) of the supernova ejecta “nebula”.

This fine sensor of the density profile can help to probe the mass of the exploding white dwarf and its kinetic energy. A clear diagnostic of low  $n_e$  comes from the emission at  $\lambda 5200 \text{ \AA}$ ,  $\lambda 4300 \text{ \AA}$ , and  $\lambda 5000 \text{ \AA}$ . These emissions are due to  $\text{Fe}^+$   $a^4\text{F}-b^4\text{P}$  and  $a^4\text{F}-a^4\text{H}$  transitions, whose lower energy terms can be significantly depopulated if  $n_e$  is low. This ratio becomes a diagnostic of ejected mass. If lower masses give on average lower collisional excitation rates for those forbidden transitions, the rates decrease significantly. Another interesting ratio of  $[\text{Fe II}]$  is that of  $a^4\text{F}-b^4\text{P}$  to  $a^4\text{F}-a^4\text{P}$ , with emissions at  $\lambda 5262$  and  $\lambda 8617 \text{ \AA}$ , though there are emissions at around  $8600 \text{ \AA}$  from other elements that can prevent the discrimination. In any case, these  $[\text{Fe II}]$  lines at long wavelength do inform on how reddened the SN Ia is. They provide an internal estimate of reddening.

The second aspect relative to the amount of  $^{56}\text{Ni}$  is that it impacts the degree of ionization and electron temperature  $T_e$  of the ejecta, which are kept warm by the thermalization of the  $\gamma$ -rays and positrons ( $e^+$ ) from the decay of  $^{56}\text{Co}$  (coming from  $^{56}\text{Ni}$ ) into  $^{56}\text{Fe}$ . While the emissivity of the different forbidden transitions of  $\text{Fe}^+$  keeps track of the electron density profile of the supernova, the ratio  $\text{Fe}^+$  to  $\text{Fe}^{++}$  gives information on  $T_e$  and the ionization of the ejecta. Since there is a large number of forbidden lines over the wavelength range at which SNe Ia are observed, there is also complementary information to obtain an internal estimate of the reddening. A good description of the ionization degree of the ejecta depends on the ionization treatment in the radiation transport code, and on factors that need evaluation, such as trapping of the positron energy, among others. A feature inherent to the density of the ejecta is that the ionization stage is kept high (more Fe III in detriment of Fe II) when the density is low and the recombination rates decrease.

A fit with a theoretical spectrum is shown in Figure 14 to illustrate the ions present and dominating the emission of SN 2011fe at a late phase.

There is a general agreement, among different authors using different codes, that sub-Chandra explosion models tend to produce overionized ejecta (Ruiz-Lapuente 1996; Mazzali et al. 2015; Wilk et al 2018, Shingles et al. 2020), though the more recent denser sub-Chandrasekhar models seem to fit as well as Chandrasekhar models the spectra of normal SNe Ia. In general, there is an overionization in the theoretical spectra calculated for all the models with the available codes and that is being currently addressed (see Shingles et al. 2022). An internal test at the nebular phase showed that the R96 code and the ARTIS code gave the same overall flux level of the nebular spectra for W7 model amongst others.

Due to the limitations to achieve a perfect fit, and the need of being extremely precise in the distance derived with spectra, a decision to proceed towards a purely empirical approach was made. This has proved to be very successful.

## B. Historical considerations

In the 90's, the use of theoretical models to infer basic properties of the SNe Ia from spectra taken at late times was proposed (see Ruiz–Lapuente 1996; Ruiz–Lapuente & Lucy 1992). The idea was to obtain at the same time the  $^{56}\text{Ni}$  mass, the reddening and the distance to the SN. Using this method, Ruiz Lapuente (1996) derived, for a reduced sample of SNe Ia, a value of the Hubble constant of  $H_0 = 68 \pm 6$  (statistical)  $\pm 7$  (systematic)  $\text{km s}^{-1} \text{Mpc}^{-1}$ . The procedure was first to measure distances to the SNe Ia, then obtain their absolute B magnitude at peak brightness and derive a fiducial absolute magnitude  $M_B$  for the SNe Ia sample. Then, this one was tied to a  $H_0$  value as in Hamuy et al. (1995):

$$\log H_0 = 0.2\{M_{\text{MAX}}^B - 1.624(\pm 0.582)[\Delta m_{15}(B) - 1.1] + 28.296(\pm 0.080)\} \quad (3)$$

Such calibration has changed dramatically since the 90's. Now the *Phillips relation* includes terms in higher orders of  $[\Delta m_{15}(B) - 1.1]$ . The derivation of  $H_0$  relies on the connection between the second and third rung in the cosmic distance ladder, i.e from SNe Ia which are not in the Hubble flow (with  $z$  well below 0.1) and those which are already in the Hubble flow. The process used by most collaborations still relies in obtaining a fiducial absolute magnitude in B of the SNe Ia at peak,  $M_B^0$ , in the local SNe Ia sample. However, such derivation needs corrections from extinction, variations of colors at peak maximum brightness in the sample, dependency with the host galaxy. In addition, to place them in the Hubble flow a reliable intercept with the SNe Ia in the Hubble flow is required. Given the complexity of this route, it is not strange to find that  $M_B^0$  varies amongst publications.

We can skip intermediate paths in this project by going to distances of twins at large enough  $z$  where peculiar velocity corrections are not needed. Then we obtain  $H_0$  directly.